

THE PENNSYLVANIA STATE UNIVERSITY  
SCHREYER HONORS COLLEGE

DEPARTMENT OF NUTRITION

TRIMETHYLAMINE N-OXIDE (TMAO) AND ATHEROSCLEROSIS: THE POTENTIAL  
ROLE OF SPECIFIC HISTONE HYPOMETHYLATION

ELISABETH BACH  
SPRING 2020

A thesis  
submitted in partial fulfillment  
of the requirements  
for a baccalaureate degree  
in Nutritional Sciences  
with honors in Nutritional Sciences

Reviewed and approved\* by the following:

Rita Castro  
Research Assistant Professor of Nutritional Sciences  
Thesis Supervisor

Alison D. Gernand  
Professor of Nutritional Sciences  
Honors Adviser

\* Signatures are on file in the Schreyer Honors College.

## ABSTRACT

**Background:** Cardiovascular disease, the global leading cause of death, is a result of atherosclerosis, a pathological condition characterized by inflammation, endothelial cell dysfunction and plaque formation in the vascular system. Increased levels of trimethylamine N-oxide (TMAO), a microbial byproduct of dietary choline, betaine, and carnitine, have been associated with atherosclerosis development; however, the molecular mechanisms which underlie this association are not fully understood. Because previous research has disclosed a link between decreased trimethylation of histone H3 on lysine 27 (H3K27me3), vascular inflammation, endothelial dysfunction, and atherosclerosis, this study aimed to determine whether the same molecular mechanism, i.e. specific histone hypomethylation, could contribute to the vascular toxicity of TMAO.

**Methods and results:** Studies were conducted on human umbilical vein endothelial cells under TMAO treatment as compared to positive and negative controls. First, the effects of TMAO on translational levels of relevant genes (associated with atherosclerosis) were assessed using real time quantitative polymerase chain reactions (RT-qPCR). Nevertheless, the obtained results were unclear, thus requiring further investigation. Afterwards, In-Cell Western blotting was used to quantify the endothelial cell content of H3K27me3, which was found to be significantly decreased by TMAO treatment (after 24 hours, in unsupplemented media). Finally, profiting from an ongoing experiment in which apoE-deficient mice were being fed either atherogenic or control diets, plasma TMAO levels from both groups were quantified. The results showed a concomitant increase in atherosclerotic plaque coverage and serum TMAO concentrations.

**Conclusions:** Overall, suppression of H3K27 trimethylation may contribute to the vascular toxicity associated with increased plasma TMAO concentrations, however, additional investigation is necessary.

## TABLE OF CONTENTS

|   |      |
|---|------|
| LIST OF FIGURES .....   | vi   |
| LIST OF TABLES .....  | vii  |
| ACKNOWLEDGEMENTS .....  | viii |
| <u>Chapter 1 INTRODUCTION</u> .....   | 1    |
| <u>1. Development of Cardiovascular Disease and Atherosclerosis</u> .....           | 1    |
| <u>1.1 Cardiovascular Disease</u> .....   | 1    |
| <u>1.2 Endothelial Dysfunction, Chronic Inflammation, and Atherosclerosis</u> ..... | 2    |
| <u>1.3 Experimental Models for the Study of Atherosclerosis</u> .....               | 5    |
| <u>2. Trimethylamine N-oxide (TMAO) and Atherosclerosis</u> .....                   | 7    |
| <u>2.1 Metabolism of Trimethylamine N-oxide</u> .....                               | 7    |
| <u>2.2 TMAO's Role in Atherosclerosis</u> .....                                     | 8    |
| <u>3. SAH and Atherosclerosis</u> .....   | 13   |
| <u>3.1 Metabolism of Homocysteine</u> .....   | 13   |
| <u>3.2 SAH and Atherosclerosis</u> .....  | 14   |
| <u>3.3 SAH's Mechanism as a Model for TMAO</u> .....                                | 15   |
| <u>Chapter 2 METHODS</u> .....  | 16   |
| <u>1. Cell Studies</u> .....  | 16   |
| <u>1.1 Cell Culture and Treatments</u> .....  | 16   |
| <u>1.2 RNA Extraction and Quantification</u> .....                                  | 17   |
| <u>1.3 Real Time Quantitative PCR Analysis</u> .....                                | 17   |
| <u>1.4 In-Cell Western</u> .....  | 18   |
| <u>1.5 Statistical Analysis</u> .....   | 19   |
| <u>2. Animal Studies</u> .....  | 19   |
| <u>2.1 Animals and Diets</u> .....  | 19   |
| <u>2.2 Blood collection and TMAO Quantification</u> .....                           | 20   |
| <u>2.3 Aorta Processing and Oil Red Staining</u> .....                              | 20   |
| <u>Statistical analysis</u> .....   | 21   |
| <u>Chapter 3 RESULTS</u> .....  | 22   |
| <u>1. Overview</u> .....  | 22   |
| <u>2. Cell Studies Results</u> .....  | 22   |
| <u>2.1 RNA Quality Checks</u> .....   | 22   |
| <u>2.2 RT-qPCR Results</u> .....  | 23   |
| <u>2.3 In-Cell Western Results</u> .....  | 28   |
| <u>3. Animal Studies Results</u> .....  | 29   |
| <u>Chapter 4 DISCUSSION AND CONCLUSIONS</u> .....                                   | 32   |

|   |    |
|---|----|
| <a href="#">1. Trimethylamine N-oxide inconsistently affected the expression of inflammatory cytokines and adhesion molecules in HUVECs</a> ..... | 32 |
| <a href="#">2. Trimethylamine N-oxide does not induce inflammation via suppression of methyltransferase expression in HUVECs</a> .....            | 33 |
| <a href="#">3. Trimethylamine N-oxide reduces HUVEC content of H3K27me3</a> .....   | 35 |
| <a href="#">4. Trimethylamine N-oxide is associated with atherosclerosis in mice</a> .....  | 35 |
| <a href="#">4. Proposed mechanism for TMAO-induced atherosclerosis</a> .....  | 35 |
| <a href="#">5. Conclusions and Future Studies</a> .....   | 36 |
| <a href="#">Chapter 5 REFERENCES</a> .....  | 37 |

## LIST OF FIGURES

|  |    |
|--|----|
| <a href="#"><u>Figure 1: Components of Atherosclerotic Plaque</u></a> .....  | 2  |
| <a href="#"><u>Figure 2: Monocyte Recruitment and Inflammation in Atherosclerosis</u></a> .....  | 4  |
| <a href="#"><u>Figure 3: Stable and Unstable Atherosclerotic Plaques</u></a> .....   | 5  |
| <a href="#"><u>Figure 4: Metabolism of Choline, Betaine, and Carnitine</u></a> .....   | 7  |
| <a href="#"><u>Figure 5: Homocysteine Metabolism</u></a> .....   | 13 |
| <a href="#"><u>Figure 6: Representative quality gel of RNA obtained from HUVECs</u></a> .....  | 23 |
| <a href="#"><u>Figure 7: TMAO's Time-dependent effect on target expression in different passages of HUVEC cells.</u></a> .....                                     | 24 |
| <a href="#"><u>Figure 8: : TMAO's time, concentration, and combination driven effect on target expression.</u></a>   | 25 |
| <a href="#"><u>Figure 9: TMAO's effect on target expression when carried in different media types.</u></a> .....   | 27 |
| <a href="#"><u>Figure 10: In-cell Western Imaging of H3K27 trimethylation under TMAO, ADA, or Control conditions in Complete or Unsupplemented media</u></a> ..... | 28 |
| <a href="#"><u>Figure 11: Oil Red Staining of Plaque in High-fat vs. Control-fed ApoE-deficient Mice</u></a> .....   | 30 |
| <a href="#"><u>Figure 12: Proposed Mechanism of Hypomethylation resulting from TMAO Concentrations</u></a>   | 36 |

**LIST OF TABLES**

|  |    |
|--|----|
| <a href="#"><u>Table 1: In Vitro Studies Investigating the Atherogenic Effects of TMAO</u></a> .....   | 11 |
| <a href="#"><u>Table 2: Animal Studies Investigating the Atherogenic Effects of TMAO</u></a> .....   | 11 |
| <a href="#"><u>Table 3: Human Studies Investigating the Atherogenic Effects of TMAO</u></a> .....  | 12 |
| <a href="#"><u>Table 4: Primer Sequences for Real Time Quantitative PCR</u></a> .....  | 18 |
| <a href="#"><u>Table 5: Control and High-Fat Diets Composition</u></a> .....   | 20 |
| <a href="#"><u>Table 6: In-Cell Western Results: H3K27me3 content in HUVEC under ADA or TMAO treatments</u></a> .....                                  | 29 |
| <a href="#"><u>Table 7: % Atherosclerotic plaque coverage and plasma TMAO concentrations in high fat vs. control-fed apoE-deficient mice</u></a> ..... | 31 |

## ACKNOWLEDGEMENTS

This thesis would not have been possible without the help of so many people around me. First, I would like to thank my thesis supervisor, Dr. Rita Castro, for working through this entire process with me. This was an entirely new experience for me, and she really helped me find my way when things were stressful or unclear, and overall provided me with a huge learning experience. I would also like to thank Dr. Alison Gernand for her patience and understanding with me throughout this process.

I would like to thank all of my lab-mates for working with me. Specifically, a huge amount of gratitude goes out to Floyd Mattie and Courtney Whalen for devoting countless hours to walking me through numerous research projects and techniques as well as providing feedback on my research and writing.

Lastly, I would like to thank my friends and family for supporting me throughout this entire process. It was very emotional and stressful at times, and needless to say I've cried on a few shoulders. They were always there to lend that shoulder and bolster me back up, and they always shared my joy in success.

## Chapter 1

### INTRODUCTION

#### 1. Development of Cardiovascular Disease and Atherosclerosis

##### *1.1 Cardiovascular Disease*

Cardiovascular disease (CVD) is an overarching term for a group of diseases caused by disorders of the heart and blood vessels including hypertension, cerebrovascular disease, coronary heart disease, and heart failure.<sup>1</sup> According to the WHO (World Health Organization), CVD accounts for over 31% mortality globally, with myocardial infarction and stroke being the most common causes of death.<sup>2</sup> Additionally, CVD is a leading cause of loss of disability-adjusted life years (DALYs), a measure of overall disease burden.<sup>3</sup> Just in the United States, CVD kills about 647,000 people each year (~ 1 in every 4 deaths), making it the leading cause of death, and costs the United States about 219 billion dollars in health care expenses and productivity losses each year.<sup>4</sup>

There are numerous lifestyle, environmental, and genetic risk factors for CVD. Lifestyle risk factors are typically modifiable, and include physical inactivity, smoking, and diet composition.<sup>5</sup> For example, dietary patterns rich in saturated fats, animal products, refined sugars, and salt are associated with increased CVD risk. Conversely, consumption of fruits, vegetables, and fiber are protective against CVD.<sup>6</sup> Unmodifiable risk factors then include having a family history of CVD, being older in age, being male, and having certain ethnicities. Other risk factors may be a result of a combination of environmental, genetic, or lifestyle factors. These include risk factors such as high LDL (low-density lipoprotein) cholesterol levels, low HDL (high-density lipoprotein) cholesterol levels, hypertension, obesity, and diabetes.<sup>5</sup>

Cardiovascular disease is seen predominantly in developed countries and is rising in developing countries, indicating that Westernized lifestyles heavily influence its development.<sup>7</sup>

Alongside industry and agricultural development, westernized populations have exhibited a significant increase in the consumption of heavily processed foods, snack foods, restaurant foods, and fast foods, all of which amplify intake of saturated fats, refined sugars, and salt.<sup>7</sup>

Additionally, developed countries tend to suffer from increasing physical inactivity.

Westernized culture has gradually adopted more and more sedentary jobs with longer commutes and work hours, leaving less time for activities and recreation.<sup>6</sup> These habits predispose individuals to the development of CVD, and these trends may in part explain the growing prevalence of this disease.

### *1.2 Endothelial Dysfunction, Chronic Inflammation, and Atherosclerosis*

Cardiovascular disease results from atherosclerosis, a condition characterized by the hardening of the blood vessels resulting from the deposition of fatty plaques as depicted in figure 1. These plaques are composed of foam cells, cholesterol particles, smooth muscle cells, and other cellular debris within the endothelial layer of the arteries.<sup>8</sup>

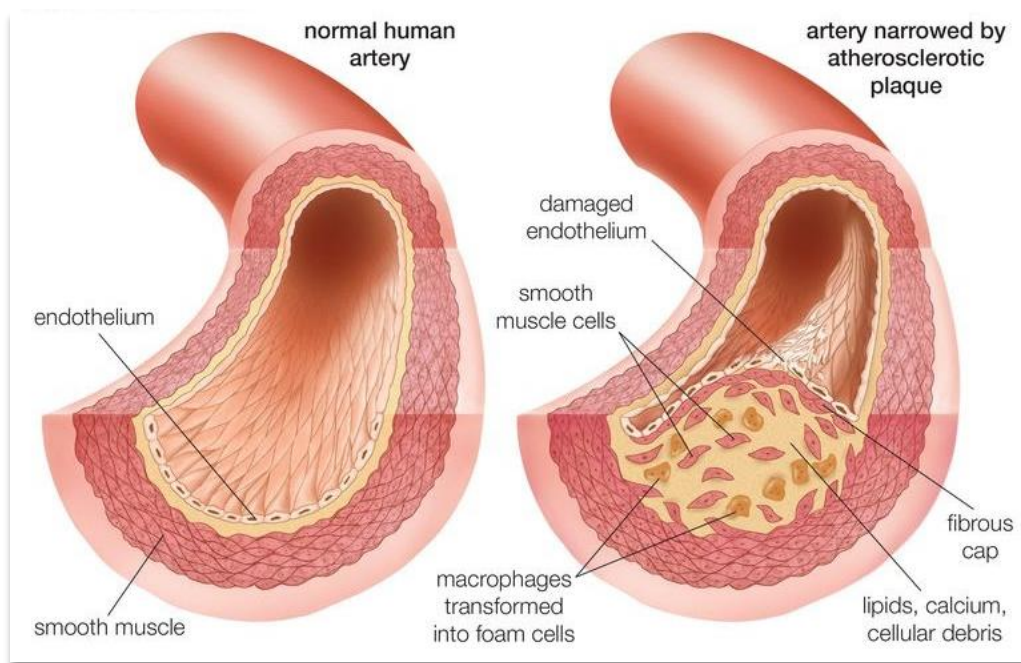


**Figure 1: Components of Atherosclerotic Plaque (from ref. 5)**

Atherosclerosis is a chronic inflammatory process that begins with the impairment of the function of endothelial cells lining the inner surface of all blood vessels. The vascular endothelium is the squamous monolayer of cells which serves as an interface between the blood and the vessel wall and is a key regulator of vascular homeostasis. Most notably, it is responsible for the production of nitric oxide (NO), a compound which regulates vascular tone. In addition to its function as a vasodilator, NO has been shown to prevent oxidation of low-density lipoproteins (LDL) and platelet aggregation, two processes involved in the establishment of vascular lesions. Alongside the regulation of NO release, the healthy endothelium also actively participates in the suppression of morphological changes that would favor the atherosclerotic process such as smooth muscle cell growth and the release of substances that regulate hemostasis (such as fibrinolytic factors).<sup>8</sup>

The term “endothelial dysfunction” refers to the impairment of these endothelial functions, which include regulation of vascular tone and homeostasis. A decrease in NO bioavailability and an impairment of cell redox balance are major features of endothelial dysfunction. As a result, endothelial dysfunction often leads to a pro-inflammatory state which then leads to the formation of atherosclerotic plaques.<sup>8</sup>

While there is a combination of environmental and genetic risk factors that play into one’s susceptibility to atherosclerosis, the formation of atherosclerotic plaque appears to have a universal pathogenesis process. First, damage to the arterial wall’s endothelial layer as a result of smoking, hypertension, or oxidization of LDL particles leads to endothelial dysfunction, thus reducing NO and disturbing previously discussed endothelial functions. This damage also allows for the accumulation of cholesterol particles beneath the endothelial cell layer. The resulting inflammatory response includes the release of cytokines such as IL-1 $\beta$  (interleukin 1B), TNF- $\alpha$  (tumor necrosis factor alpha), and IL-8 (interleukin 8) which are responsible for recruiting monocytes to the damaged site.<sup>9,10</sup>

Adhesion molecules such as ICAM-1 (intercellular adhesion molecule 1), VCAM-1 (vascular cell adhesion molecule 1), and E-selectin on the surface of the endothelial cells help the monocytes migrate across the endothelial lining,<sup>11</sup> where they then differentiate into macrophages.<sup>9,10</sup> These macrophages will phagocytize the accumulating LDL particles and consequently become foam cells, as depicted in figure 2. Foam cell enlargement due to

cholesterol accumulation then causes further inflammation which, in positive feedback loop, leads to continued monocyte recruitment and continued foam cell formation.<sup>10</sup> This accumulation forms a fatty streak composed of LDL particles, cellular debris, and foam cells underneath the endothelium and is considered the first stage of atherosclerotic plaque development. As these plaques grow, they begin to restrict the flow of blood and further weaken the arterial wall.<sup>12</sup>

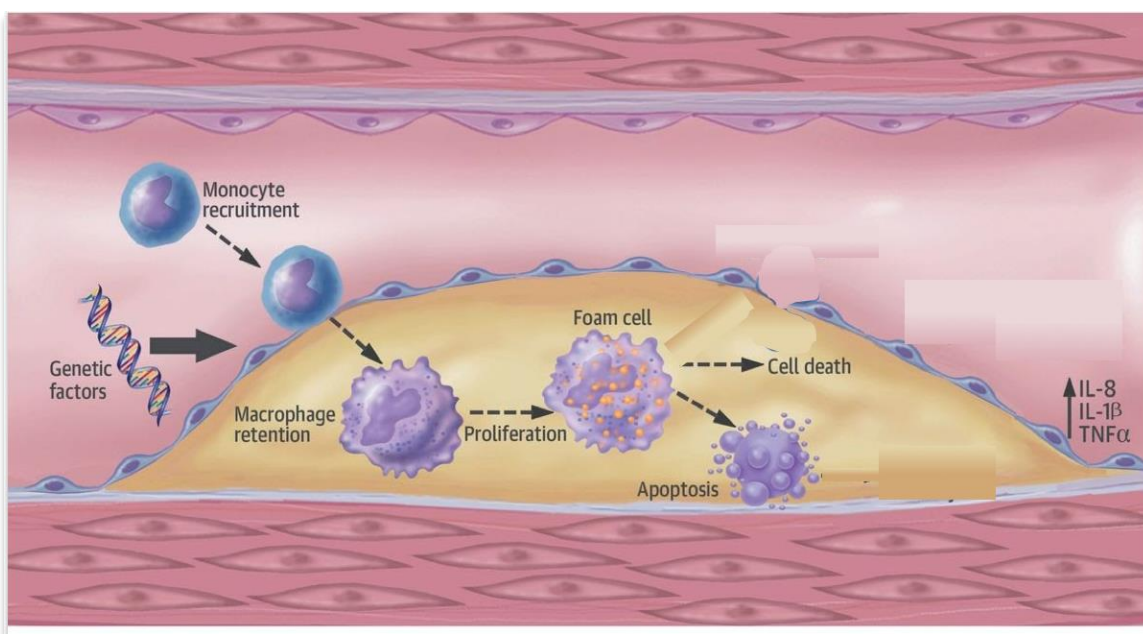


**Figure 2: Monocyte Recruitment and Inflammation in Atherosclerosis (adapted from ref. 13):** IL-1 $\beta$  (Interleukin 1 beta), IL-8 (Interleukin 8), TNF- $\alpha$  (Tumor necrosis factor alpha)

The accumulation of plaque stimulates the migration of vascular smooth muscle cells (depicted in figure 1) into the vascular intima. These smooth muscle cells produce fibrous tissues and extracellular matrix, which form a fibrous cap on the lumen-facing surface of the plaque.<sup>12</sup> Fully formed atherosclerotic plaques will maintain calcified, fibrous caps composed primarily of these extracellular matrix components and migrating smooth muscle cells.<sup>14</sup> Tissues in the middle of fully developed atherosclerotic plaques are often restricted from nutrients and will become necrotic. As the necrotic core grows, it begins to destroy surrounding tissues, including the tissues of the fibrous cap.<sup>12</sup>

Different plaque compositions carry different levels of risk for adverse cardiovascular events. As depicted in figure 3, stable plaques have a very thick fibrous cap and a relatively small lipid core with minimal macrophage content. Contrarily, unstable plaques have a thin, weak fibrous cap, a large lipid core, and a high macrophage content.<sup>15</sup> A thin fibrous cap is more easily eroded by necrotic tissues and inflammatory factors, and is thus susceptible to rupture.<sup>12</sup> Plaque rupture results in the release of the highly thrombotic contents of the necrotic core, and the formation of clots at the site of rupture. These clots may occlude blood flow causing vascular accidents such as heart attacks, strokes, or varying levels of tissue damage.<sup>16</sup>

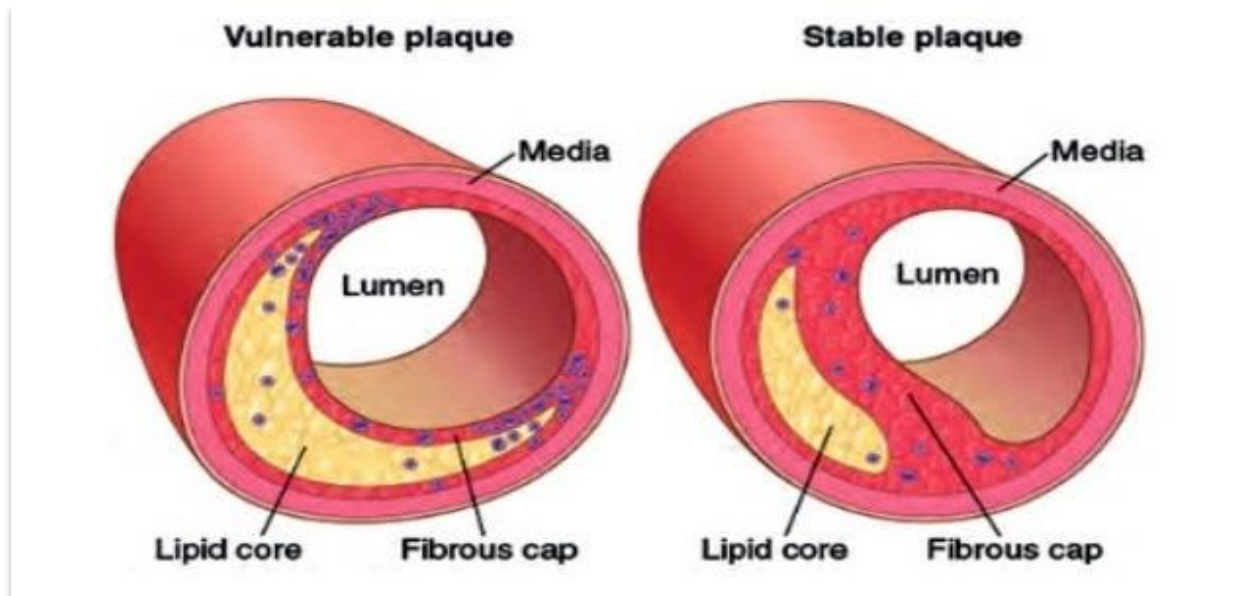


Figure 3: Stable and Unstable Atherosclerotic Plaques (from ref. 17)

### 1.3 Experimental Models for the Study of Atherosclerosis

Several experimental models of the human vascular system are used to study human atherosclerosis.

In vitro models consist of cultured human vascular endothelial cells used to simulate the human vascular endothelium. As referred to above, the vascular endothelium is the single layer of endothelial cells that coats the entire vascular system and actively participates in vascular

homeostasis. The most widely used cells are umbilical vein endothelial cells (HUVECs) or human aortic endothelial cells (HAECs).<sup>18</sup> HUVECs in particular, sourced from healthy, postnatal umbilical veins, serve as a good model because they are easily available at a low cost.<sup>19</sup> As such, HUVECs are frequently used to investigate molecular mechanisms underlying inflammation and endothelial dysfunction.<sup>20</sup>

For in vivo models, mice have become the predominant species used to study experimental atherosclerosis because of their rapid reproduction, easy maintenance, and ease of genetic manipulation. More importantly, they are used because many of the critical processes involved in the development of atherosclerosis are shared between mice and humans. Nevertheless, differences in plasma lipid profile and in the spontaneous occurrence of vascular lesions do exist between humans and mice.<sup>21</sup> In humans, cholesteryl ester transfer protein (CETP) promotes the transfer of cholesteryl esters from anti-atherogenic HDLs to pro-atherogenic apolipoprotein B (apoB)-containing lipoproteins (such as low-density lipoprotein, LDL and very low-density lipoprotein, VLDL). However, mice lack this CETP and thus transport the cholesterol mostly in anti-atherogenic high-density lipoprotein (HDL) molecules. Additionally, mouse bile presents a higher lipophilic activity than human bile, thus reducing the intestinal absorption of cholesterol. As a result, mice do not accumulate the same levels of the atherogenic lipoproteins as humans, and thus do not naturally develop atherosclerosis within a reasonable time-frame.<sup>22</sup>

These differences are accounted for by inducing a state of hypercholesterolemia, which can be achieved by eliminating either the *apolipoprotein E (apoE)* or the *LDL receptor (LDLR)* genes.<sup>21,22</sup> Apolipoprotein E (apoE) is responsible for the efficient clearance of diet-derived chylomicrons and lipoproteins, and, the LDL receptor plays a major role in the clearance of apoE-containing lipoproteins. Thus, knocking down the expression of *apolipoprotein E (apoE)* or the *LDL receptor (LDLR)* genes in mice induces poor lipoprotein clearance with subsequent accumulation of cholesterol ester-enriched particles in the blood, which in turn promotes the development of atherosclerotic plaques.<sup>21</sup> Moreover, the progression of atherosclerosis is greatly accelerated when these mice are fed a high-fat and high-cholesterol diet. As a result, apoE-deficient and LDLR-deficient mice accumulate atherosclerotic plaques in the aorta and thus are the most widely-used in vivo models for the study of human atherosclerosis.<sup>22</sup>

## 2. Trimethylamine N-oxide (TMAO) and Atherosclerosis

### 2.1 Metabolism of Trimethylamine N-oxide

One molecule which has been shown to induce endothelial cell dysfunction and inflammation is trimethylamine N-oxide (TMAO). TMAO is an odorless, organic compound. In marine life, TMAO confers protective effects by stabilizing cellular proteins under adverse temperature, salinity, high urea, and hydrostatic pressure. However, in humans, increased plasma TMAO concentrations have been associated with a decline in vascular health.<sup>23</sup>

Plasma TMAO concentrations typically result from the consumption dietary compounds such as choline, betaine, or carnitine primarily found in animal-sourced foods (meat, eggs, poultry, dairy, and fish).<sup>23-25</sup> During digestion, certain gut microbiota in the small intestine convert these dietary compounds into trimethylamine (TMA).<sup>23,25</sup> Upon intestinal absorption, TMA is transported to the liver where flavin monooxygenases 1 and 3 (FMOs 1 and 3) oxidize TMA to TMAO as depicted in figure 4.<sup>24</sup> Following its oxidation in the liver, TMAO circulates in the bloodstream before being excreted in the urine.<sup>23-25</sup>

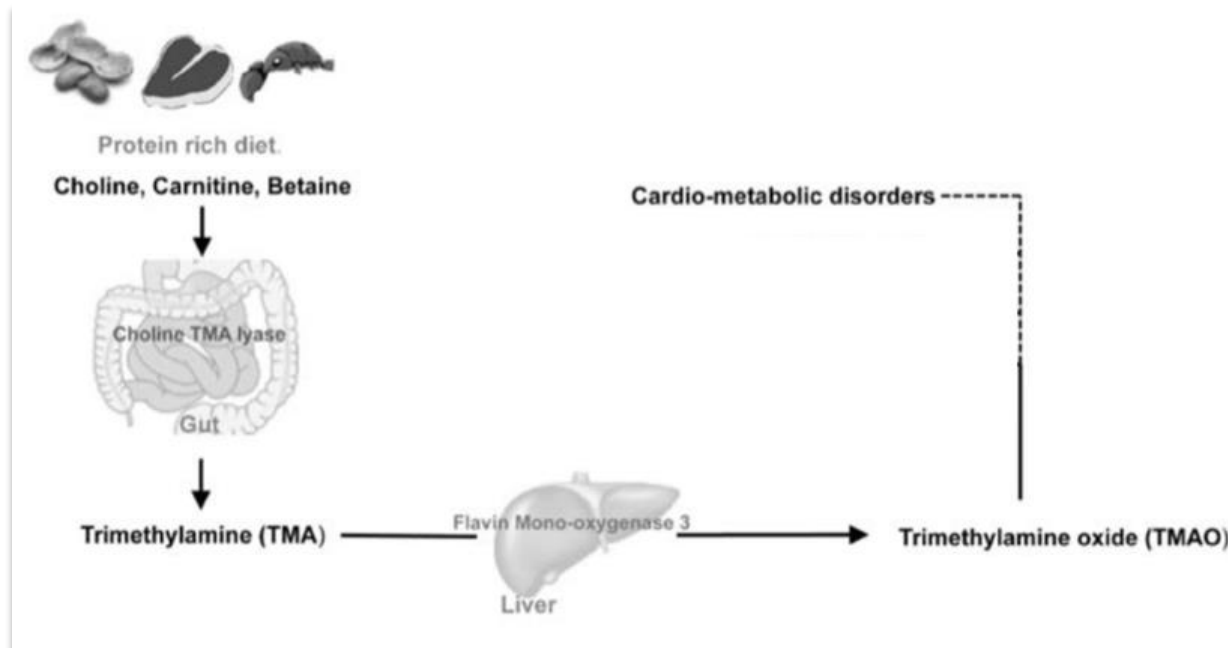


Figure 4: Metabolism of Choline, Betaine, and Carnitine (adapted from ref. 26)

The plasma level of TMAO is determined by several factors including diet, gut microbial flora, and hepatic flavin monooxygenase (FMO) activity. Studies have shown that the consumption of L-carnitine, betaine, or choline leads to increased plasma levels of TMAO. As a result, diets rich in animal products which contain high levels of these compounds have been shown to increase plasma TMAO concentrations in humans.<sup>26,43</sup> Alternatively, increasing plant-based foods may protect against this effect. One study shows that vegans/ vegetarians exhibit a much lower spike in plasma TMAO concentrations when fed L-carnitine than omnivores. This is thought to be because the intestinal microbiota involved in the conversion of carnitine to TMA (prior to absorption) are not supported by a plant-based diet.<sup>44</sup>

With regards to FMO activity, circulating concentrations of TMAO are affected by biological sex due to differences in the expression of FMO 3 and 1 isoforms (in mice and humans). In fact, human and mouse females express predominantly the more active isoform FMO3 whereas FMO3 expression in males is significantly reduced. Thus, females being more effective in oxidizing TMA to TMAO than males are more exposed to the atherogenic effects associated with excessive choline, betaine, or carnitine consumption.<sup>27,28</sup> Despite this difference,

the negative vascular effect associated with increased plasma TMAO has been documented in both males and females.<sup>27</sup>

## 2.2 TMAO's Role in Atherosclerosis

Increased plasma TMAO concentrations have been shown by multiple studies to disturb vascular homeostasis both *in vitro* and *in vivo*.

*In Vitro Studies:* Studies with HUVECs and HAECs have shown that increased TMAO concentrations induce a pro-atherogenic phenotype by promoting inflammation and up-regulation of adhesion molecules. A summary of these studies is shown in table 2. More specifically, several authors documented a TMAO-induced, increased expression of inflammatory cytokines such as IL-1 $\beta$ , TNF- $\alpha$ , and IL-8, as well as an up-regulation of the adhesion molecules ICAM-1, VCAM-1, and E-selectin.<sup>29-33</sup> Additionally, the functional relevance of the (TMAO-induced) increased expression of adhesion molecules was confirmed by showing an increase in monocyte adhesion in endothelial cells following TMAO treatment.<sup>30</sup>

Furthermore, TMAO has been shown to activate the NF- $\kappa$ B (nuclear factor kappa-light-chain-enhancer of activated B cells) pro-inflammatory pathway, which is responsible for regulating the transcription of several genes encoding for cytokine production.<sup>33,34</sup> TMAO treatments have also been shown to induce oxidative stress and reduce nitric oxide production, which contributes to endothelial dysfunction and thus atherosclerosis.<sup>29-31</sup>

*Animal Studies:* Similarly, studies performed on apoE-deficient and LDLR-deficient mice have been corroborating the atherogenic effect of TMAO. A summary of animal studies is shown in table 3. For example, upon dietary enrichment with TMA, choline, or intravenous administration of TMAO, mice exhibited increased vascular inflammation (IL-1 $\beta$ , TNF- $\alpha$ , and NF- $\kappa$ B activation) and up-regulation of adhesion molecules (ICAM-1, VCAM-1, and E-selectin).<sup>30,33,35,36</sup> Moreover, studies reported that increased plasma TMAO led to an increase in vascular lesions and atherosclerotic plaque deposition in the mice's aortas.<sup>30,36</sup>

*Human Studies:* While there are very few experimental studies on humans to corroborate that TMAO directly promotes atherosclerosis, increased plasma TMAO levels in humans have

been associated with a number of adverse cardiovascular events in several observational studies. For example, plasma TMAO concentrations have been associated with increased risk of plaque rupture,<sup>37</sup> ischemic and non-ischemic heart failure,<sup>38</sup> as well as increased mortality in ischemic stroke.<sup>39</sup> Plasma TMAO levels have also been associated with increased markers of vascular inflammation. Pro-inflammatory monocyte concentration,<sup>40</sup> tissue factor expression (involved in NF- $\kappa$ B activation), and subsequent NF- $\kappa$ B translocation<sup>34</sup> were all correlated with plasma TMAO concentrations. Additionally, TMAO has been correlated with cardiometabolic risk factors like high levels of LDL,<sup>40</sup> low levels of HDL, and low phospholipids,<sup>41</sup> and has been used as an indicator of CVD risk.<sup>42</sup> These findings are summarized in table 3.

Overall, mouse and cell studies have been reporting TMAO to be an atherogenic molecule. Moreover, observational evidence in human studies also suggests that TMAO is a pro-inflammatory molecule that negatively affects vascular homeostasis. However, the molecular mechanisms underlying the potential vascular toxicity of TMAO are not fully understood.

**Table 1: In Vitro Studies Investigating the Atherogenic Effects of TMAO**

| Source | Cell type | TMAO Concentrations ( $\mu\text{M}$ ) | Incubation Time (hours) | Results  | Outcomes  |
|--------|-----------|---------------------------------------|-------------------------|--|---|
| 29     | HUVEC     | 100, 200, 300                         | 1, 3, 6                 | <ul style="list-style-type: none"> <li>↑ oxidative stress,</li> <li>↑ IL-1<math>\beta</math> &amp; IL-18</li> <li>↓ NO production</li> </ul>   | Inflammation & endothelial cell dysfunction   |
| 30     | HUVEC     | 150, 300, 600, 900 or 600             | 24 or 0, 4, 12, 24      | <ul style="list-style-type: none"> <li>↑ IL-1<math>\beta</math>, ICAM</li> <li>↑ adhesion of monocytes</li> <li>↑ oxidative stress</li> </ul>  | NLRP3 inflammasome activated by TMAO, TMAO also induced oxidative stress  |
| 31     | HUVEC     | 0, 10, 50, 100                        | 6 and 24                | <ul style="list-style-type: none"> <li>↑ VCAM-1,</li> <li>↑ activation of NF-<math>\kappa</math>B,</li> <li>↑ activation of PKC,</li> <li>↓ HUVEC self-repair</li> </ul>                         | TMAO promotes atherosclerosis by accelerating endothelial dysfunction, decreasing self-repair, and increasing monocyte adhesion |
| 32     | HAEC      | 30                                    | 12                      | <ul style="list-style-type: none"> <li>↑ IL-1<math>\beta</math>,</li> <li>↑ activation of NLRP3 inflammasome</li> </ul>  | TMAO activates the NLRP3 inflammasome thus leading to endothelial cell dysfunction  |
| 33     | HAEC      | TMA media (concentration unknown)     | Unknown                 | <ul style="list-style-type: none"> <li>↑ IL-6, TNF-<math>\alpha</math></li> <li>↑ E-selectin, ICAM-1</li> <li>↑ Recruitment of Leukocytes</li> <li>No effect on macrophage expression</li> </ul> | NF- $\kappa$ B is a likely contributory mechanism for TMAO-dependent enhancement in atherosclerosis                             |
| 34     | HCAEC     | 10-200                                | 5                       | <ul style="list-style-type: none"> <li>↑ NF-<math>\kappa</math>B signaling pathway</li> <li>↑ Tissue Factor activity</li> <li>↑ Thrombin production</li> </ul>                                   | TMAO promoted thrombosis by promoting tissue factor expression and activity   |

Table 2: Animal Studies Investigating the Atherogenic Effects of TMAO

| Source | Animals                                      | Treatment                                     | Length (weeks) | Results   | Outcomes  |
|--------|--|---|----------------|---|---|
| 30     | Female apoE-deficient mice (8-wk old)        | 1% choline chow                               | 16             | ↑ plaque in aorta<br>↑ IL-1 $\beta$ , ICAM-1  | TMAO induced vascular inflammation and atherogenic effects  |
| 35     | Male apoE-deficient mice                     | 0.3% TMAO chow                                | 32             | ↑ fat mass<br>↑ serum lipid concentration,<br>↑ atherosclerosis<br>↓ hepatic bile acid synthesis  | TMAO induced atherosclerosis by altering bile acid profiles   |
| 36     | Male apoE-deficient mice (8-wk old)          | 1 mM TMAO water                               | 8              | ↑ atherosclerotic plaque<br>↑ TNF- $\alpha$ , IL-6<br>↑ ICAM-1  | TMAO promotes atherosclerosis and CD36/MAPK/JNK pathways may be involved  |
| 33     | Female LDLR-deficient mice (8-wk old)        | 1.3% choline water or 86 mmol TMAO injections | 3              | ↑ TNF- $\alpha$ ,<br>↑ ICAM1, E-selectin<br>↑ monocytes in choline fed<br>↑ NF- $\kappa$ B,<br>activation of PKC,<br>↑ IL-6,<br>↑ E-selectin, ICAM1 in injected group | Chronic choline feeding leads to vascular inflammation<br>Acute TMAO injection activates inflammatory signaling and gene expression |
| 40     | Non-genetically manipulated mice (10-wk old) | 1.3% choline chow                             | 3              | ↑ CD14 and CD16 monocyte levels<br>↑ Ly6C <sup>high</sup> monocytes   | TMAO caused increases in pro-inflammatory monocytes   |

**Table 3: Human Studies Investigating the Atherogenic Effects of TMAO**

| Source | Subjects                                       | Diet/<br>Treatment<br>(if any) | Length<br>(if any) | Results  | Outcome  |
|--------|--|--------------------------------|--------------------|--|--|
| 37     | Patients w/<br>myocardial<br>infarction        | --                             | --                 | High plasma TMAO levels<br>correlate w/ plaque rupture   | TMAO may be a biomarker<br>for plaque rupture  |
| 38     | Patient w/<br>chronic<br>heart failure<br>(HF) | --                             | --                 | Plasma TMAO associated<br>most strongly w/ ischemic<br>HF, then stable CAD, then<br>non-ischemic heart disease               | TMAO is associated with<br>disease severity and lower<br>survival in HF patients         |
| 39     | Patients w/<br>Ischemic<br>Stroke              | --                             | --                 | TMAO associated w/<br>↓ functional outcome and<br>↑ mortality  | TMAO levels may predict<br>unfavorable outcomes in<br>acute ischemic stroke<br>patients  |
| 40     | Patients w/<br>Ischemic<br>Stroke              | --                             | --                 | TMAO associated w/<br>↑ risk of adverse<br>cardiovascular event and<br>↑ CD14 <sup>++</sup> / CD16 <sup>+</sup><br>monocytes | TMAO may increase pro-<br>inflammatory monocytes<br>and risk of cardiovascular<br>events |
| 41     | Varied<br>health status                        | --                             | --                 | TMAO associated w/<br>↓ HDL and phospholipids<br>↓ methylation potential<br>↑ instance of diabetes                           | TMAO concentrations are<br>associated with an advanced<br>cardiometabolic risk profile   |
| 42     | Patients w/<br>CVD                             | --                             | --                 | TMAO associated w/<br>Future risk of CVD   | TMAO helps predict risk of<br>CVD beyond use of only<br>traditional risk factors         |

### 3. SAH and Atherosclerosis

#### 3.1 Metabolism of Homocysteine

Homocysteine is a molecule involved in one-carbon metabolism where it is formed by methionine demethylation. Methionine is first converted to SAM (S-adenosylmethionine), which then donates its methyl group to several methyltransferases thus forming SAH (S-adenosylhomocysteine). SAH can then be further hydrolyzed to homocysteine, which can then be either catabolized by the transsulfuration pathway or remethylated back to methionine via two independent pathways.<sup>45,46</sup> This process is further illustrated in figure 5.

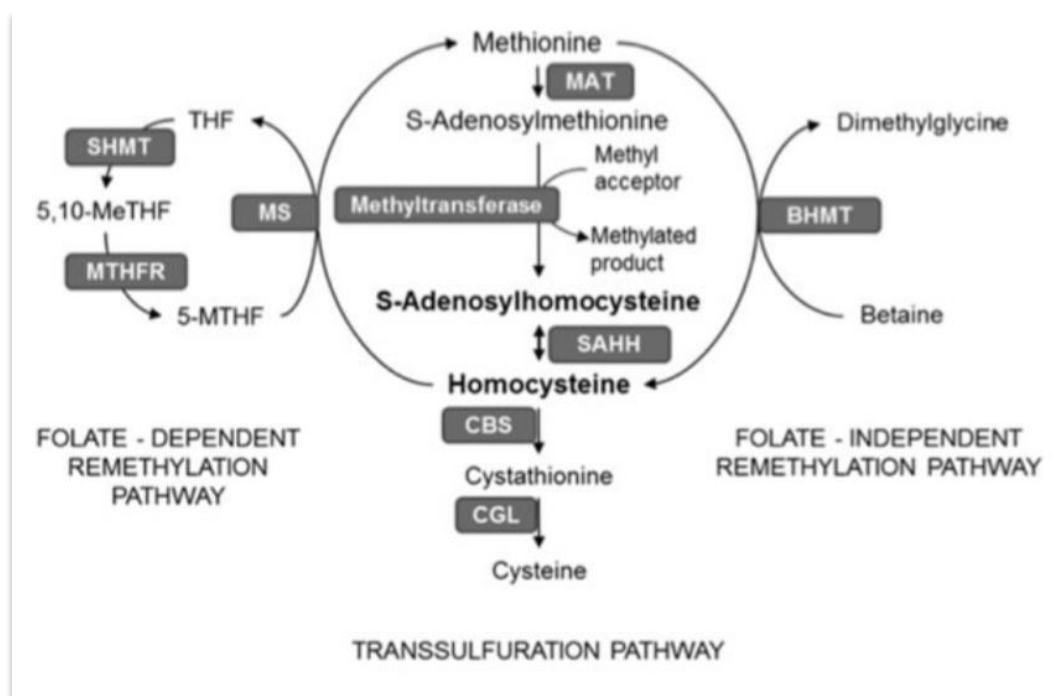


**Figure 5: Homocysteine Metabolism (from ref. 45, 46):** Homocysteine is formed from methionine, via S-adenosylmethionine (the main methyl donor compound) and S-adenosylhomocysteine (SAH), by the action of methionine adenosyltransferase (MAT) and SAH-hydrolase (SAHH). Once formed, homocysteine can enter the transsulfuration pathway or be remethylated into methionine by two different remethylation pathways. In the folate-dependent remethylation pathway, methionine synthase assisted by its cofactor vitamin B12 (methylcobalamin) transfer a methyl group from 5-MTHF (5-methyltetrahydrofolate) to the homocysteine molecule forming methionine and tetrahydrofolate (THF). SHMT (serine hydroxymethyltransferase) will then convert the remaining THF to 5,10-MeTHF (5,10-methylenetetrahydrofolate), which is then converted by MTHFR (methylene tetrahydrofolate reductase) back to 5-MTHF, that will assist in the remethylation of a new molecule of homocysteine. In the liver and kidney, remethylation can occur via the folate-independent remethylation pathway, in which BHMT (betaine-homocysteine methyltransferase) catalyzes the transfer of a methyl group from betaine to homocysteine thus forming methionine. In the transsulfuration pathway, CBS (cystathionine B-synthase) and its cofactor vitamin B6 (pyridoxal

*phosphate) condenses homocysteine and serine to cystathionine which is then converted to cysteine by CGL (cystathionine  $\gamma$ -lyase). Cysteine is then used in the synthesis of glutathione, proteins, or further metabolized and excreted in the urine.*

Several non-genetic (such as B-vitamin deficiency) and genetic factors (such as cystathionine B-synthase or MTHFR deficiencies) lead to hyperhomocysteinemia, a condition marked by chronically elevated plasma concentrations of homocysteine.<sup>45</sup>

### *3.2 SAH and Atherosclerosis*

Hyperhomocysteinemia is considered a common and independent risk factor for CVD.<sup>47</sup> Analyses have shown that an increase of 5  $\mu\text{mol/L}$  in plasma homocysteine leads to a 20% increase in CVD risk,<sup>48</sup> but the vascular toxicity of homocysteine is most likely due to concomitant increases in its precursor, SAH. Accordingly, SAH has been shown to be a more accurate marker of CVD risk than homocysteine.<sup>49</sup>

SAH accumulation disturbs the balance of methylation processes in one carbon metabolism. As discussed above, SAM is an important methyl donor for a variety of methyltransferases. These methyltransferases methylate a wide variety of targets including DNA, RNA, and proteins. Most importantly, because SAH has a very similar structure to that of SAM, SAH acts as a competitive inhibitor of these SAM-dependent methyltransferases. Consequently, the accumulation of SAH leads to hypomethylation of several SAM-dependent targets, including nuclear histones whose methylation status regulates gene expression.<sup>45</sup>

EZH2 (enhancer zest homolog 2), EHMT1 (euchromatic histone lysine methyltransferase 1), and EHMT2 (euchromatic histone lysine methyltransferase 2) are examples of SAM-dependent methyltransferases responsible for histone methylation. EZH2 specifically has been shown to catalyze the trimethylation of histone 3 lysine 27 (H3K27me3) which negatively regulates gene expression. This epigenetic tag suppresses the expression of genes involved in the inflammatory process and endothelial dysfunction that, as previously mentioned, are involved in the establishment and progression of atherosclerosis.<sup>50</sup> More specifically, our previous *in vitro* studies showed that excess SAH accumulation decreases EZH2 expression and

activity, lessening the methylation of endothelial H3K27me3, and thus promoting an atherogenic phenotype.<sup>50</sup>

### *3.3 SAH's Mechanism as a Model for TMAO*

As discussed above, SAH has been shown to promote specific histone hypomethylation and promote an atherogenic endothelial phenotype. Specifically, our previous studies showed that, in HAECs, SAH accumulation decreases H3K27me3 methylation, thus upregulating the expression of genes which encode inflammatory cytokines (IL-1 $\beta$ , TNF- $\alpha$ ) and adhesion molecules (VCAM-1, ICAM-1, E-selectin).<sup>50,51</sup> These are all key molecular processes involved in the development of atherosclerosis. As discussed in section 2.2, the same inflammatory phenotype has been observed in response to TMAO treatments in similar models, although the underlying mechanism is not entirely solved. Moreover, TMAO has been associated with hypomethylation in humans, which favors the possibility that TMAO may also decrease histone methylation (H3K27) as a part of its inflammatory mechanism.<sup>41</sup> Based on our observations, we sought to:

1. Confirm the pro-atherogenic phenotype induced by TMAO in cultured human endothelial cells.
2. Investigate whether or not TMAO induces specific histone hypomethylation, unveiling a new molecular mechanism contributing to the atherogenic properties of TMAO.

## **Chapter 2**

### **METHODS**

The methods described here include all of the collaborative work completed in Dr. Rita Castro's lab. For this thesis, I specifically completed all cell studies. Regarding the animal studies, I assisted Dr. Rita Castro's team in the care and maintenance of the mice, blood collection, and Oil Red O staining of aortas.

#### **1. Cell Studies**

##### *1.1 Cell Culture and Treatments*

Pooled human umbilical vein endothelial cells (HUVECs) from healthy subjects were obtained from Lifeline Cell Technology and were cultured in culture medium (VascuLife) supplemented with 5% FBS (fetal bovine serum), 5 ng/mL rh FGF (recombinant human fibroblast growth factors), 15 ng/mL rh IGF-1 (recombinant human insulin-like growth factor 1), 5 ng/mL rh EGF (recombinant human epidermal growth factor), 5 ng/mL rh VEGF (recombinant human vascular endothelial growth factor), 0.75 U/mL heparin sulfate, 50 µg/mL ascorbic acid, 1 µg/mL hydrocortisone hemisuccinate, and 10 mM L-glutamine (VascuLife). Cells were grown under humidified 5% CO<sub>2</sub> conditions until 80-90% confluence was reached. HUVECs were then passaged at a 1:3 ratio by trypsin dissociation (Corning, 0.05% trypsin, 0.53 mM EDTA).

Experiments were performed using cells between 3 and 11 passages grown to 70-90% confluence. Treatments with TMAO were performed using several final concentrations (100 or 500 µM). Moreover, treatments with adenosine-2-3-dialdehyde (ADA, 20 µM), an SAHH inhibitor (figure 5), were used to increase the intracellular levels of the hypomethylating metabolite SAH, and were used as positive controls. The ability of ADA treatment to

significantly increase intracellular SAH and to promote an atherogenic phenotype in human endothelial cells has been previously reported by us.<sup>50,52</sup> In addition, incubations were also performed in the absence of TMAO or ADA and were used as negative controls. Treatments were performed in a variety of different medias (complete media, media without FBS or growth factors, media without FBS, or media without growth factors) for varying incubation periods (4 to 72 hours).

All cell manipulations were executed in a SterilGard Class II Type A/B3 Laminar flow hood (The Baker Company).

### *1.2 RNA Extraction and Quantification*

Cells were lysed using RLT Buffer (Qiagen) containing 1%  $\beta$ -mercaptoethanol. RNA extraction was then performed using an RNeasy RNA extraction kit (Qiagen) following manufacturer protocol including the optional on-column DNase I treatment for removal of genomic DNA contamination. RNA was then quantified using the NanoDrop 2000C (Thermo Scientific) and RNA quality was evaluated based on ribosomal RNA (rRNA) integrity using a bleach gel (1% agarose, 1% bleach, Tris-acetate EDTA (TAE) gel).<sup>53</sup> The presence of both 28S and 18S rRNA bands with very minimal or no smearing was considered indicative of good quality RNA.

### *1.3 Real Time Quantitative PCR Analysis*

RNA samples were diluted to 50 ng/uL or 100 ng/uL as was appropriate and reverse transcribed using M-MLV reverse transcriptase (Promega) with oligo dT primers (Promega). Resulting cDNAs were then diluted to 10 ng/uL and 2 ng/uL based on RNA input of reverse transcription reaction. Real time quantitative PCR (RT-qPCR) was performed using 10 uL Perfecta SYBR Green SuperMix (Quantabio), 5 uL of primer combo (1  $\mu$ M), and 5 uL of cDNA (2 ng/uL or 10 ng/uL for VCAM-1 and IL-1 $\beta$  targets) in each well. Samples were run on a StepOnePlus Real-Time PCR System (Applied Biosystems) and thermocycler stages were as

follows: Initial denature at 95°C for 3 minutes (1 cycle), denature/aneal/extend at 95°C for 15 seconds, 59°C for 15 seconds, 72°C for 20 seconds (40 cycles), final extension at 72°C for 2 minutes (1 cycle), and a melt curve cycle. Results were analyzed using the relative quantification application (RQ) within the Thermofisher online analysis suite. Primer sequences for all studied transcripts are listed in Table 3. B2M and GAPDH were used as endogenous controls.

RT-qPCR results and relative quantification (delta delta CT method) calculations were performed within the Thermofisher Connect cloud-based suite of analysis tools using the relative quantification application (RQ). As compared to control samples, changes of greater than 1 (double) or less than -1 (half) on a log(2) scale were considered relevant whereas quantified values falling between -1 and 1 were considered to be below the detection limitations of our assay.

**Table 4: Primer Sequences for Real Time Quantitative PCR**

| Primer | Forward Sequence 5'→3'        | Reverse Sequence 5'→3'         |
|--------|-------------------------------|--------------------------------|
| ICAM1  | 5'-GAGCTTCGTGTCCTGTATGG-3'    | 5'-TCCAGTTTCCCGGACAATCC-3'     |
| VCAM1  | 5'-TGGACATAAGAAACTGGAAAAGG-3' | 5'-GATTTCTGGATCTCTAGGGAATGA-3' |
| EZH2   | 5'-ACGCTTTTCTGTAGGCGATG-3'    | 5'-CTTTGCTCCCTCCAAATGCTG-3'    |
| EHMT1  | 5'-CTACTTCTGCACAGCGGGTA-3'    | 5'-GGGGACAATAGCTGGCGTTA-3'     |
| EHMT2  | 5'-ACACCATTGACAGCTCAGGG-3'    | 5'-GAGCTTCTTCCGCCTCTCTG-3'     |
| IL-1B  | 5'-GCTCGCCAGTGAAATGATGG-3'    | 5'-CTGGAAGGAGCACTTCATCTGT-3'   |
| B2M    | 5'-GATGAGTATGCCTGCCGTGT-3'    | 5'-CTGCTTACATGTCTCGATCCCA-3'   |
| GAPDH  | 5'-GGTTTCTATAAATTGAGCCCGCA-3' | 5'-CCCAATACGACCAAATCCGTTG-3'   |

#### 1.4 In-Cell Western

HUVECs were seeded into 96 well plates at levels near confluence (based on well-surface area) and allowed to attach for 2 hours. Cells were then treated with TMAO (500 µM), ADA (20 µM), or vehicle (Phosphate Buffered Saline, PBS) dissolved in complete media or media without FBS/growth factors for varying time periods (6 or 24 hours). Cells were fixed using 10% Neutral Buffered Formalin (NBF) for 15 minutes before being washed/permeabilized

with 1x PBS + 0.1% Triton X-100 washing solution. Cells were blocked with Intercept Blocking Buffer (Li-Cor) for 1.5 hours with gentle shaking. Cells were then incubated overnight at 4°C with rabbit anti-H327Kme3 (Epigentek) at a 1:200 ratio in Intercept Blocking Buffer. Cells were then washed with PBS +0.1% Tween 20 (PBS-T) and incubated in donkey anti-rabbit IgG-IR Dye 800 CW (Li-Cor) at 1:250 ratio and Cell Tag 700 stain (Li-Cor) at a 1:300 ratio. Cells were again washed with PBS-T. Relative histone methylation levels (Cell Tag) were then evaluated by measurement of fluorescence intensity on an Odyssey CLX Infrared Imaging System (Li-Cor).

### *1.5 Statistical Analysis*

Real time quantitative PCR: A  $\geq 2$ -fold increase and  $\geq 50\%$  reductions in RNA expression levels were considered significant based on analysis thresholds.

In-Cell Westerns: The results presented as mean  $\pm$  standard error of mean (SEM). For comparison of two treatments, unpaired Student's T-test was used. Analyses were performed in GraphPad Prism 7 (GraphPad Software, La Jolla, CA, USA), with statistical significance level set to 0.05.

## **2. Animal Studies**

### *2.1 Animals and Diets*

Seven-week-old apoE<sup>-/-</sup> mice (Jackson Laboratory, Bar Harbor, ME) were used in this study. The animals were maintained in a room at  $22 \pm 2^\circ\text{C}$  with a 12-h light-dark cycle with free access to water. Mice were feed ad libitum, during 12 weeks, with one of the following diets prepared based on AIN 93M recommendations but with different levels of fat and cholesterol (Research Diets, New Brunswick, NJ). A control diet (C, 5% w/w fat, n= 3 animals), and a High Fat diet (HF, 20% w/w fat and 0.15% cholesterol, n= 5 animals). Details about the diet composition are shown in table 5. Diets were refreshed on a weekly basis, at which time animals and remaining food were weighed. All procedures were performed in compliance with the

Institutional Animal Care and Use Committee of the Pennsylvania State University, which specifically approved this study.

**Table 5: Control and High-Fat Diets Composition**

|                               | <b>Control Diet</b> | <b>High Fat Diet</b> |
|-------------------------------|---------------------|----------------------|
| Protein (% kilocalories)      | 18.5                | 18.4                 |
| Carbohydrate (% kilocalories) | 70.2                | 41.6                 |
| Fat (% kilocalories)          | 11.3                | 39.9                 |
| Cholesterol (% per g)         | 0                   | 1.25                 |

### *2.2 Blood collection and TMAO Quantification*

After 8 weeks on each diet, blood was collected from the retro-orbital cavity into heparinized tubes and immediately put on ice. Within 30 minutes, plasma was isolated by centrifugation at 4°C and stored at -80°C until TMAO quantification.

TMAO quantification was performed at the Center of Metabolomics, Baylor Scott & White Research Institute, Dallas, Texas, USA using triple quadrupole mass spectrometry.

### *2.3 Aorta Processing and Oil Red Staining*

After 12 weeks, mice were euthanized by carbon dioxide inhalation, and after the exposure of the aorta, 10 mL of cold PBS were perfused through the left ventricle of the heart. The aorta and heart were then removed and perfused with 10% neutral buffered formalin (NBF) in PBS via the left ventricle. Tissue was fixed in 10% NBF overnight, washed with PBS, and subjected to Oil Red O staining, as described below.

Fixed aortas were stained with Oil Red O (EMD chemicals, Cat. #3125-12) to facilitate complete adventitial fat removal during dissection. Briefly, aortas were dehydrated in successive methanol - water solutions (25%, 50%, 78% at 15 minutes each, Room Temperature (RT), rocking). Aortas were then incubated in Oil Red O working solution (5 parts 2.8% Oil Red O in

methanol : 2 parts 1M sodium hydroxide, twice filtered, 0.45um) for 2 hours at RT, rocking. Aortas were then washed and rehydrated with successive methanol-PBS solutions (78%, 78%, 50%, 25%, PBS only, PBS only, at 15 minutes each, RT, rocking), then stored at 4oC until dissection. Tissues surrounding aortas were dissected away under a stereomicroscope using 0.10mm minutien pins (Austerlitz), #55 Dumont forceps (Roboz), and micro dissecting spring scissors, taking care to remove as much adventitial fat as possible. The attached top of heart along with aortic root were removed. Cleanly dissected aortas were again stained with Oil Red O to completely stain atherosclerotic plaques.<sup>54</sup> Aortas were pinned out intact and photographed on each side. From these photographs, percent plaque coverage was estimated using FIJI.<sup>55</sup>

### *Statistical analysis*

The results are presented as mean  $\pm$  standard error of mean (SEM). Unpaired Student's T-test was performed to compare differences between the two groups of animals, with the accepted value of  $P < 0.05$  as significant, using GraphPad Prism 7 (GraphPad Software, La Jolla, CA, USA).

## **Chapter 3**

### **RESULTS**

#### **1. Overview**

We conducted our studies using in vitro and in vivo models of atherosclerosis. These results first outline the TMAO-induced effects on the transcriptional levels of relevant targets in HUVECs using real time quantitative polymerase chain reactions (RT-qPCR), and using treatment-induced SAH accumulation as positive controls. We quantified the effects of TMAO on the expression levels of inflammatory cytokines (IL-1B), adhesion molecules (ICAM-1, VCAM-1), and histone methyltransferases (EZH2, EHMT1, EHMT2). Next, these results present the translational effects of TMAO treatment. We used In-Cell Western techniques to quantify the TMAO-induced impact on HUVEC H3K27me3 content. SAH accumulation was again induced as a positive control for these experiments. Finally, apoE-deficient mice were fed an atherogenic diet or control diet in order to disclose whether TMAO levels would correlate with plaque accumulation. These results display the quantified circulating TMAO levels and the concomitant amount of atherosclerotic plaque in the mice aortas.

#### **2. Cell Studies Results**

##### *2.1 RNA Quality Checks*

Ribosomal RNA (rRNA) quality checks were performed prior to cDNA synthesis using gel electrophoresis. An example of one gel is shown below in figure 6. Samples were loaded at equal volumes, not equal RNA concentrations, so band intensity is not indicative of quality (concentrations were normalized prior to subsequent cDNA synthesis). 28S and 18S rRNA

bands were well-defined across all groups and experiments, indicating that RNA samples presented good quality and would be used in cDNA synthesis.

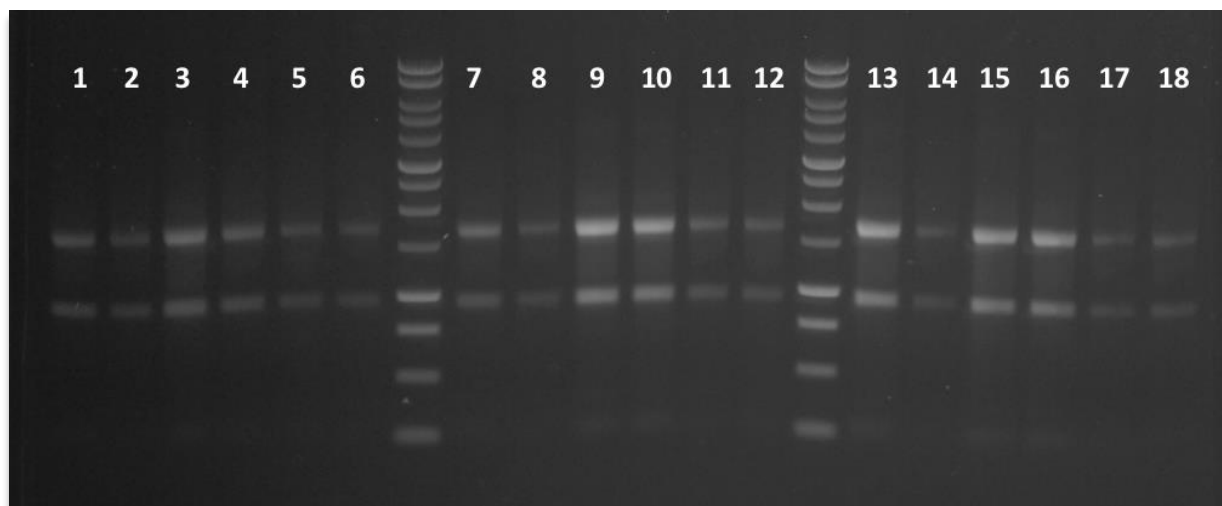


**Figure 6: Representative quality gel of RNA obtained from HUVECs** grown in the following conditions: 1. Control 24 hr, 2. ADA 24 hr, 3. TMAO 100 24 hr, 4. TMAO 500 24 hr, 5. ADA + TMAO 100 24 hr, 6. ADA + TMAO 500 24 hr, 7. Control 48 hr, 8. ADA 48 hr, 9. TMAO 100 48 hr, 10. TMAO 500 48 hr, 11. ADA + TMAO 100 48 hr, 12. ADA + TMAO 500 48 hr, 13. Control 72 hr, 14. ADA 72 hr, 15. TMAO 100 72 hr, 16. TMAO 500 72 hr, 17. ADA + TMAO 100 72 hr, 18. ADA + TMAO 500 72 hr. Well-defined 28S and 18S ribosomal RNA bands are indicative of good RNA quality. Lanes vary in intensity as samples were analyzed prior to RNA quantification and so lane intensities only represent the varying concentrations of the RNA preparations, not RNA integrity. RNA concentration was normalized prior to later use.

## 2.2 RT-qPCR Results

The relative expression levels of pro-inflammatory molecules IL-1 $\beta$ , VCAM-1, and ICAM-1 in TMAO-treated cells was determined via RT-qPCR. Likewise, relative expression levels of the following methyltransferases were also quantified: EZH2 (enhancer of zest homolog 2), EHMT1 (eurochromatic histone lysine methyltransferase 1), and EHMT2 (eurochromatic histone lysine methyltransferase 2). The obtained results are shown in figures 7-9.

For the first set of RT-qPCR experiments, HUVECs were incubated with TMAO (100  $\mu$ M) and ADA (20  $\mu$ M) for periods of 4, 12, or 24 hours, and were compared to controls (figure

7). TMAO treatment at 24 hours resulted in a significant increase in the expression levels of all targets (EHMT1, EHMT2, EZH2, ICAM-1, IL-1 $\beta$ ) except for VCAM-1. However, TMAO increased VCAM-1 expression by 8-fold after 12 hours of incubation (P06 group), but by 24 hours returned to insignificant expression levels. Concerning the effects of ADA treatment, a significant increase in ICAM-1, after 24 hours, and IL-1 $\beta$ , at all time points, was observed.

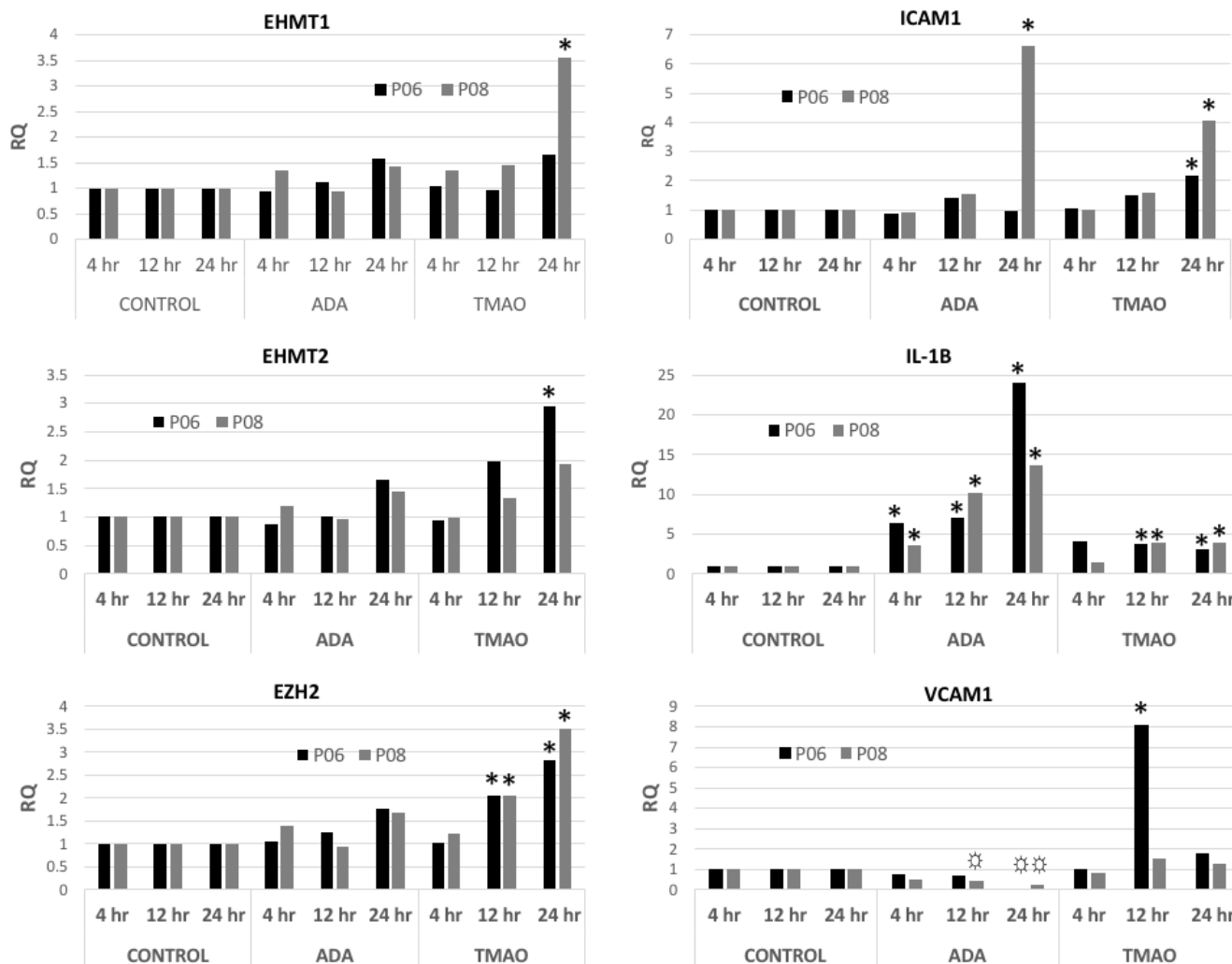


**Figure 7: TMAO's Time-dependent effect on target expression in different passages of HUVEC cells. \*indicates  $\geq 2$ -fold increase in expression, ☼ indicates  $\geq 50\%$  reduction in expression.**

The previous set of experiments (figure 7) suggested that TMAO could affect the expression of several targets after longer incubation times, so for the second set of RT-qPCR experiments, the treatment duration was lengthened to 24, 48, and 72 hours. In this second set of

cell experiments, new concentrations of TMAO (100  $\mu$ M and 500  $\mu$ M) were used, and coincubation studies were also performed. Specifically, treatments involved TMAO at either concentration (TMAO 100 and TMAO 500) or TMAO at either concentration coincubated with ADA (ADA+TMAO 100 and ADA+TMAO 500). Results from this set are shown in figure 8. In this set of treatments, TMAO was shown to have no significant effects on any of the targets, thus failing to confirm our previous results. Significant differences seen in the TMAO + ADA groups were entirely ADA-driven. Additionally, ADA treatments halved EHMT1 expression at 24 hours, but had no effect at 48 or 72 hours. ADA also increased ICAM-1 expression by more than 40-fold at 48 and 72 hours, and IL-1 $\beta$  expression by 44-fold by 72 hours with similar, apparently ADA-driven, results in the ADA + TMAO combination groups.

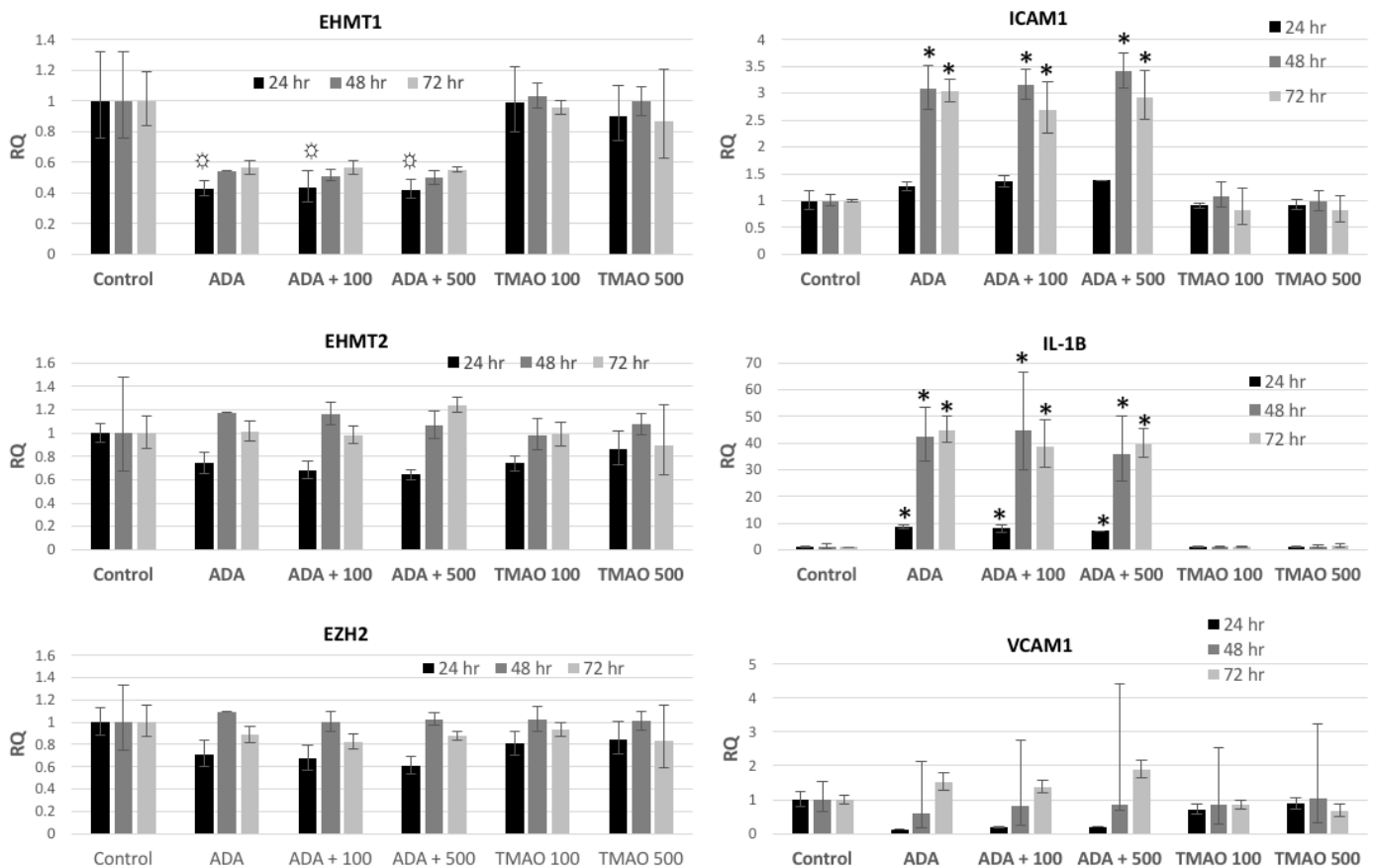


**Figure 8: : TMAO's time, concentration, and combination driven effect on target expression.** Error bars indicate 95% confidence that the mean lies within those values. \*indicates  $\geq 2$ -fold increase in expression, ☼ indicates  $\geq 50\%$  reduction in expression

Thus, in the second set of RT-qPCR experiments (figure 8), we confirmed ADA's positive effect on ICAM-1 and IL-1 $\beta$  expression. However, we were unable to observe any effect of the TMAO treatments, which was inconsistent with the first set of results (TMAO increased expression at 24 hours for nearly all targets, figure 7). To exclude any potential interfering role of the media components, treatments were administered in complete media as well as media without FBS (No FBS), media without growth factors (no GF), or unsupplemented media (No FBS/GF). Cells were incubated in treatments for either 6 or 24 hours due to time constraints. Results from this experiment are shown in figure 9. Compared to respective controls, neither TMAO nor ADA had any significant effect on EHMT1, EHMT2, or EZH2 expression regardless of media type or incubation period. TMAO induced a 2.5-fold increase in ICAM-1 expression in the No GF group at 6 hours, but beyond that, TMAO appeared to have no significant effect on ICAM-1 expression. Additionally, TMAO decreased expression of IL-1 $\beta$  and VCAM-1 over 50% in a majority of the media types. No consistent changes were seen as a result of the varying media types. Moreover, ADA significantly increased IL-1 $\beta$  and ICAM-1 by at least 2-fold after 24 hours of incubation.

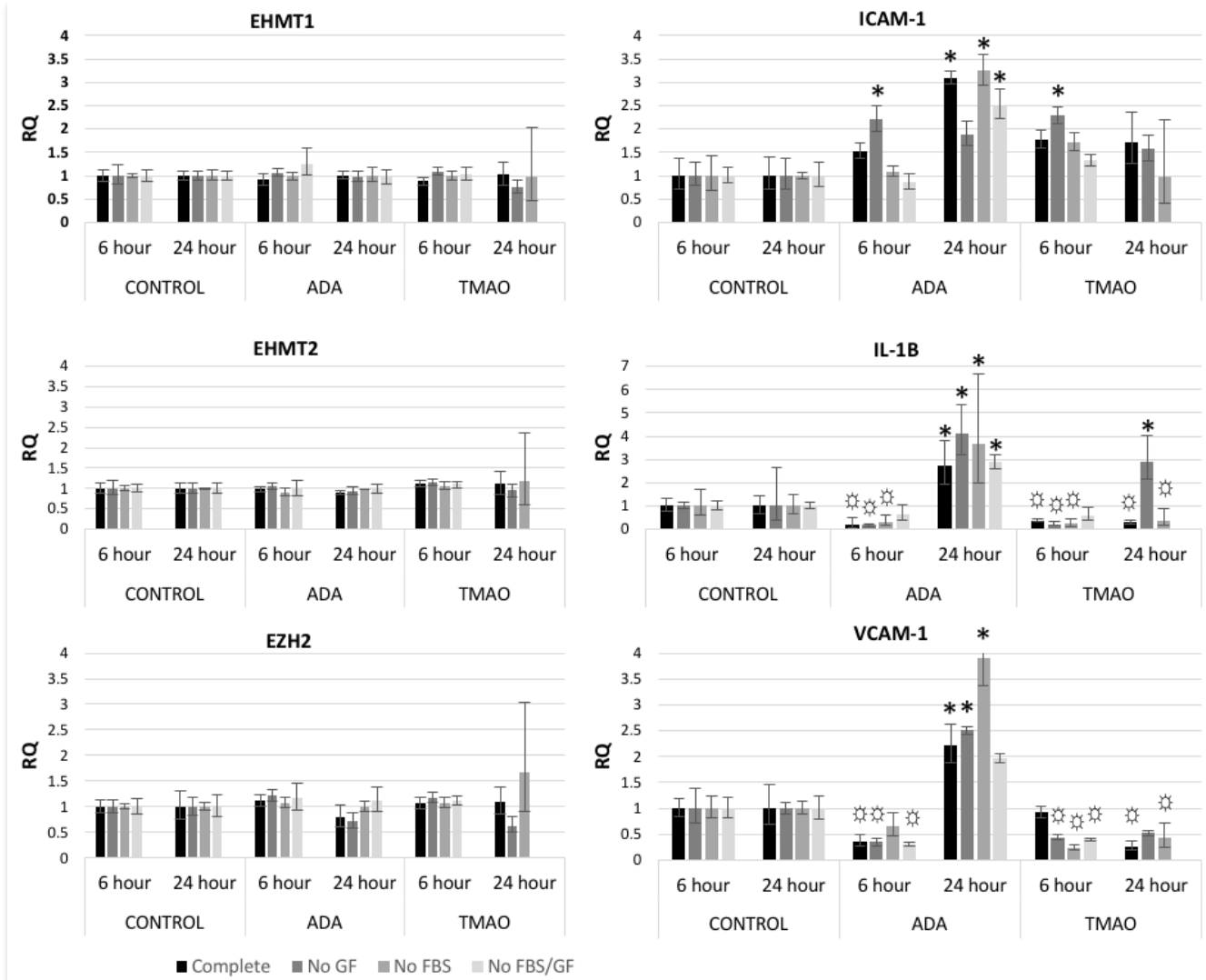


**Figure 9: TMAO's effect on target expression when carried in different media types.** All data points relative to time and media type matched controls. Error bars indicate 95% confidence that the mean lies within those values. \*indicates  $\geq 2$ -fold increase in expression, ⚙️ indicates  $\geq 50\%$  reduction in expression

While we were able to confirm ADA's positive effect on ICAM-1 and IL-1 $\beta$  expression after 24 hours, there were inconsistencies regarding the effects of TMAO treatment which warranted additional investigation. With this purpose, we performed a new set of HUVEC incubation studies with TMAO (500  $\mu$ M) and ADA (20  $\mu$ M) for 6 or 24 hours using complete media as vehicle. Subsequently, we collected RNA for a fourth round of RT-qPCR experiments.

Unfortunately, however, due to the policies surrounding the COVID-19 outbreak, we were unable to access the lab and conduct the final RT-qPCR studies.

### 2.3 In-Cell Western Results

In-cell Western blots were performed to determine whether or not TMAO had a specific histone hypomethylating effect on HUVECs in vitro. Because the RT-qPCR results were altered slightly by media types, fully supplemented (complete) and unsupplemented medias were used as treatment vehicles in the in-cell Western blots. A representative imaging of the blots can be seen in figure 10.

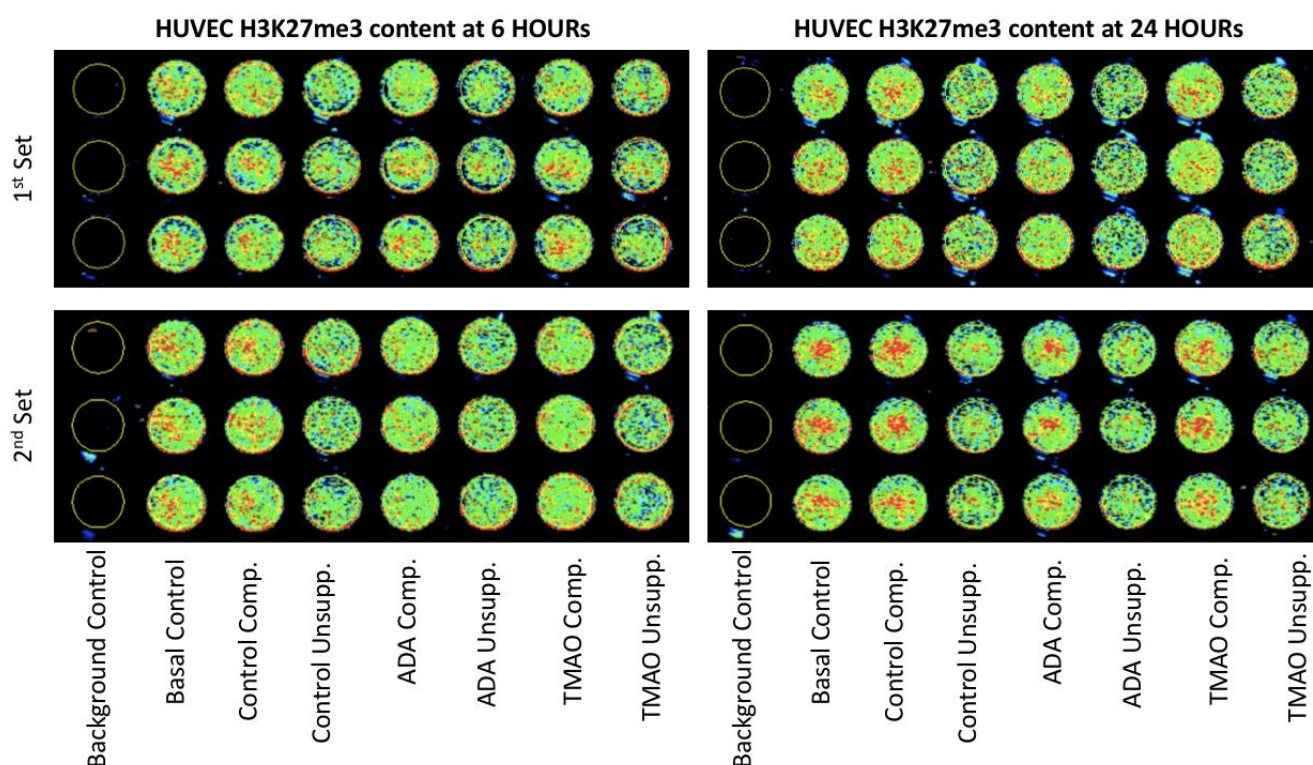


**Figure 10: In-cell Western Imaging of H3K27 trimethylation under TMAO, ADA, or Control conditions in Complete or Unsupplemented media**

Compared to their respective controls, 6-hour TMAO treatments, either using complete or unsupplemented media, had no influence on the HUVEC content of H3K27me3 methylation at 6 hours. When TMAO was supplied in complete media, there was no major effect on

methylation at 24 hours. However, in unsupplemented media at 24 hours, TMAO significantly decreased H3K27me3 content ( $p=0.015$ , Student's T-test).

ADA induced slight, but insignificant, decreases in specific trimethylation of histone H3K27 after six hours (9.6% decrease in complete media, 7.65% decrease in unsupplemented media). At 24 hours, ADA induced similar decreases (7.25%) in complete media. More importantly, at 24 hours in the unsupplemented media, ADA led to much more significant decreases, reducing H2K27 content by 26.6% ( $p=0.004$ , Student's T-test). These results are shown in table 6.

**Table 6: In-Cell Western Results: H3K27me3 content in HUVEC under ADA or TMAO treatments**

| <b>HUVEC relative H3K27me3 content after 6 HOUR (% ICW)</b>  |                          |                      |                       |                             |                      |                       |
|--|--------------------------|----------------------|-----------------------|-----------------------------|----------------------|-----------------------|
|  | <b>Complete Media</b>    |                      |                       | <b>Unsupplemented Media</b> |                      |                       |
|  | <b>Control<br/>(n=3)</b> | <b>ADA<br/>(n=3)</b> | <b>TMAO<br/>(n=3)</b> | <b>Control<br/>(n=3)</b>    | <b>ADA<br/>(n=3)</b> | <b>TMAO<br/>(n=3)</b> |
| 1 <sup>st</sup> Set  | 100                      | 85.3 ± 4.3           | 94.9 ± 2.8            | 100                         | 78.7 ± 3.1           | 90.8 ± 5.6            |
| 2 <sup>nd</sup> Set  | 100                      | 95.5 ± 4.3           | 106 ± 0.7             | 100                         | 106 ± 1.8            | 105 ± 5.1             |
| <b>Average</b>   | <b>100</b>               | <b>90.4</b>          | <b>100.45</b>         | <b>100</b>                  | <b>92.35</b>         | <b>97.9</b>           |
| <b>HUVEC relative H3K27me3 content after 24 HOUR (% ICW)</b> |                          |                      |                       |                             |                      |                       |
|  | <b>Complete Media</b>    |                      |                       | <b>Unsupplemented Media</b> |                      |                       |
|  | <b>Control<br/>(n=3)</b> | <b>ADA<br/>(n=3)</b> | <b>TMAO<br/>(n=3)</b> | <b>Control<br/>(n=3)</b>    | <b>ADA<br/>(n=3)</b> | <b>TMAO<br/>(n=3)</b> |
| 1 <sup>st</sup> Set  | 100                      | 94.2 ± 1.0           | 98 ± 0.7              | 100                         | 89 ± 5.6             | 90.9 ± 4.4            |
| 2 <sup>nd</sup> Set  | 100                      | 91.3 ± 3.2           | 94 ± 2.3              | 100                         | 57.8 ± 5.2           | 36.3 ± 8.2            |
| <b>Average</b>   | <b>100</b>               | <b>92.75</b>         | <b>96</b>             | <b>100</b>                  | <b>73.4</b>          | <b>63.6</b>           |

### 3. Animal Studies Results

Profiting from an ongoing animal experiment in the lab where apoE-deficient mice were being fed either an atherogenic-high-fat or a control diet, we sought to investigate whether we could establish a correlation between the amount of aortic atherosclerosis and the circulating

TMAO concentrations. The results are presented in figure 11 where the lipid-rich plaques are dyed red. Mice fed the high-fat diets developed significantly ( $p=0.00004$ , Student's T-test) more aortic atherosclerotic plaque ( $24.2 \pm 5.6\%$ ) than controls ( $0.02 \pm 0.1\%$ ). Moreover, high-fat-fed mice presented significantly ( $p=0.013$ , Student's T-test) higher plasma TMAO levels ( $2.80 \pm 1.12 \mu\text{M}$ ) than the control mice ( $0.017 \pm 0.006 \mu\text{M}$ ). The percentage of aortic plaque coverage in relation to the total area of aortic tissue is expressed numerically in table 7.

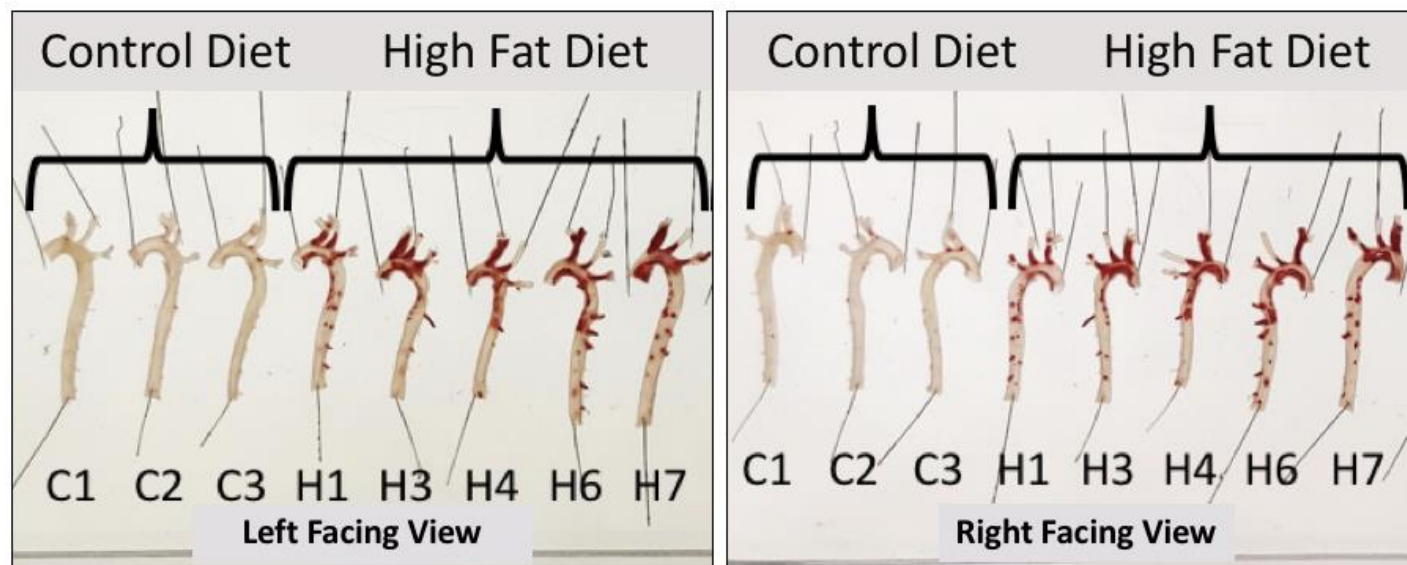


Figure 11: Oil Red Staining of Plaque in High-fat vs. Control-fed ApoE-deficient Mice

**Table 7: % Atherosclerotic plaque coverage and plasma TMAO concentrations in high fat vs. control-fed apoE-deficient mice**

| <b>% Aortic Plaque Coverage</b>   |                            |
|-----------------------------------|----------------------------|
| <b>Control (% plaque)</b>         | <b>High Fat (% plaque)</b> |
| 0.2                               | 14.3                       |
| 0.5                               | 26.1                       |
| 0.7                               | 25.2                       |
|                                   | 27.9                       |
|                                   | 27.7                       |
| <b>Average=0.4 ± 0.25</b>         | <b>Average=24.2 ± 5.66</b> |
| <b>Plasma TMAO Concentrations</b> |                            |
| <b>Control (μM)</b>               | <b>High Fat (μM)</b>       |
| 0.017 ± 0.006                     | 2.80 ± 1.12                |

## Chapter 4

### DISCUSSION AND CONCLUSIONS

TMAO has been shown to have numerous negative effects on vascular health including the promotion of inflammation and endothelial dysfunction, but the underlying mechanisms are still elusive.<sup>29-42</sup> In this study, we investigated whether TMAO would induce specific histone hypomethylation as part of its mechanism for vascular toxicity. Histone hypomethylation (as a result of SAH accumulation) has been demonstrated to produce inflammatory phenotypes in the human endothelium, increasing cytokine expression and activating the pro-inflammatory NF- $\kappa$ B pathway.<sup>50</sup> Therefore, we tested whether TMAO played a role in specific histone hypomethylation by assessing TMAO's effect on trimethylation of H3K27me3 content in HUVECs. We also explored the TMAO-induced inflammatory phenotype and investigated whether TMAO had any effect on methyltransferase expression, whose downregulation would subsequently induce histone hypomethylation.

#### *1. Trimethylamine N-oxide inconsistently affected the expression of inflammatory cytokines and adhesion molecules in HUVECs*

Before focusing on specific histone methylation, we attempted to confirm the existence of a pro-atherogenic phenotype in response to TMAO treatments in HUVECs.

Adhesion molecules (such as ICAM-1 and VCAM-1) are expressed on the vascular endothelium to facilitate monocyte entry into the intima of the arterial wall. Subsequently, these monocytes develop into lipid-phagocytizing macrophages, thus contributing to the progression of atherosclerosis.<sup>9-11</sup> As such, adhesion molecule expression is an important endothelial phenotype that contributes to plaque development. In our cell studies, we observed TMAO to have varying effects on adhesion molecule expression. In the first set of RT-qPCR experiments, TMAO treatment induced an upregulation of the expression of the adhesion molecules ICAM-1 and

VCAM-1 after 24 or 12 hours respectively. However, in the second set of experiments, TMAO had no effect on adhesion molecule expression. In the third set of experiments, TMAO appeared only to induce an increase in ICAM-1 expression at only one time-point (6 hours) and only in the growth factor-deficient media. Alternatively, VCAM-1 expression experienced a significant reduction in expression (6 and 24 hours) following TMAO treatment. However, in the studies shown in table 1, TMAO consistently upregulated adhesion molecule expression and subsequent monocyte adhesion.<sup>30-32</sup> Because we saw promising results in the first set of experiments, we question whether something interfered with the TMAO treatments in the subsequent experiments. However, we do not suspect that this interference was due to solubility issues as TMAO dissolved rapidly in all solutions.

Pro-inflammatory cytokines (such as IL-1 $\beta$ ) are another set of molecules that contribute to the atherosclerotic process. In fact, atherosclerosis is considered a disease of chronic inflammation, in which cytokines' expression is upregulated, signaling the migration and activation of immune cells to the disturbed endothelium. In atherosclerosis, cytokine expression is often upregulated.<sup>9,10</sup> Accordingly, TMAO has been shown by previous studies to upregulate cytokine expression (table 1), specifically IL-1 $\beta$ , expression, thus contributing to atherosclerosis progression.<sup>29,32,33</sup> However, in our cell studies, TMAO appeared to inconsistently affect cytokine expression. Our first set of cell experiments resulted in a significant increase in IL-1 $\beta$  expression at 12 and 24 hours. However, in the subsequent set of experiments, a similar result was only observed when TMAO was administered for 24 hours in growth factor-deficient media. Again, these results indicated the possibility that something interfered with TMAO treatments in the second and third round of experiments.

## *2. Trimethylamine N-oxide does not induce inflammation via suppression of methyltransferase expression in HUVECs*

Because in previous studies TMAO and SAH accumulation induced very similar atherogenic phenotypes, we questioned whether TMAO and SAH would share a similar molecular mechanism. Specifically, SAH accumulation was shown to reduce the methylation capacity of EZH2, a methyltransferase involved in the regulation of inflammation-relevant,

epigenetic methylation (H3K27me3). As a result, SAH accumulation leads to a decrease in H3K27me3 content thus upregulating the expression of genes coding for inflammatory cytokines and adhesion molecules. With this in mind, we were interested in exploring whether or not TMAO affected EZH2 expression, thereby inducing the same hypomethylating effects which result from SAH accumulation. Additionally, we investigated TMAO's effect on EHMT1 and EHMT2 expression. These are two additional methyltransferases involved in the suppression of inflammation. EHMT1 and EHMT2 are responsible for regulating the NF- $\kappa$ B inflammatory pathway, and thus a decrease in their expression due to TMAO treatments might explain how TMAO upregulates the NF- $\kappa$ B pathway.<sup>57,58</sup>

However, our cell studies did not show that TMAO had any consistent, significant effects on methyltransferase expression. In the first set of experiments, TMAO appeared to actually increase, instead of decrease, methyltransferase expression at 24 hours, which would indicate that TMAO's effect is anti-inflammatory instead of pro-inflammatory. However, in subsequent experiments, these observations were not confirmed. Based on these results, it is unlikely that TMAO achieves its inflammatory effect via EZH2, EHMT1, or EHMT2 suppression. Nevertheless, TMAO may induce hypomethylation via other mechanisms beyond the suppression of methyltransferase expression. For example, TMAO may inhibit methyltransferase function or may affect histone methylation via a different pathway. Moreover, TMAO may simply affect the expression of other methyltransferases that were not studied in these experiments.

The inconsistency of our results indicated that there are still factors that need to be accounted for in the experimental process. It is possible that cells were experiencing stress of some kind during growth, which perhaps increased basal inflammatory marker expression thus overwhelming the effects of TMAO. In the groups treated in different media types, it is possible that the shock from changing media types during treatment caused variances in the metabolic response to TMAO and ADA treatments. Replication of these experiments would allow us to determine what factors may be interfering with the consistency of our results.

### *3. Trimethylamine N-oxide reduces HUVEC content of H3K27me3*

In-cell Western results showed a considerable decrease in H3K27 trimethylation after 24 hours of TMAO treatment in unsupplemented media. Interestingly, ADA, our positive control, also exhibited its greatest reductive effects at the 24-hour point in unsupplemented media. An SAH-induced decrease in H3K27me3 target has been shown in previous studies (with regard to SAH accumulation) to increase cytokine (IL-1 $\beta$ ) expression, which then activates the NF- $\kappa$ B pathway and upregulates inflammatory genes.<sup>50</sup> Consequently, our results suggest that TMAO may induce a portion of its inflammatory effects via specific histone hypomethylation. However, whether or not this histone hypomethylation translates into endothelial dysfunction and inflammation could not be confirmed by our RT-qPCR experiments.

### *4. Trimethylamine N-oxide is associated with atherosclerosis in mice*

Finally, we investigated plasma TMAO levels in two groups of apoE-deficient mice presenting significantly different levels of atherosclerosis. As mentioned in Chapter 1, section 1.3, apoE deficient mice accumulate lipid-rich atherosclerotic plaques in their aortas (which is a measure of the extent of atherosclerosis). Using Oil Red O staining, we visualized and quantified the amount of plaque which accumulated in aortas from mice fed either an atherogenic or control diet. The results showed that in the aortas from mice fed a control diet, only about 0.4% of the vessel was covered with plaques. However, in the high-fat-fed mice aortas, about a quarter of the vessels was covered in plaques (24.2%). Interestingly, control mice also presented significantly lower plasma TMAO levels than the high-fat animals thus suggesting that TMAO may be an atherogenic molecule. However, these results were observational, and thus no causative assumptions could be made from this data.

### *4. Proposed mechanism for TMAO-induced atherosclerosis*

Overall, based on the results of this study, we hypothesized that TMAO, via a currently unknown mechanism, induces specific histone hypomethylation by decreasing the endothelial

content of the epigenetic tag H3K27me3. This would cause an upregulation of IL-1 $\beta$  expression. Interestingly, this pro-inflammatory cytokine is both an NF- $\kappa$ B activator and an NF- $\kappa$ B target. Thus, IL-1 $\beta$  upregulation could contribute to NF- $\kappa$ B activation and the vascular inflammatory response that promotes atherosclerosis progression. An illustration of this proposed mechanism can be seen in figure 12.

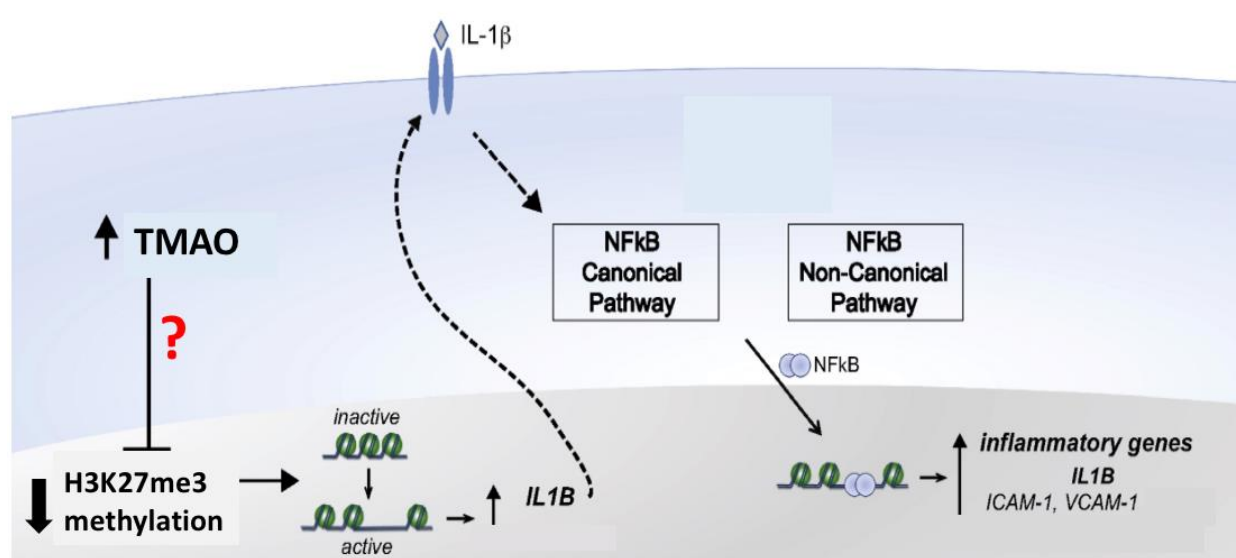


Figure 12: Proposed Mechanism of Hypomethylation resulting from TMAO Concentrations (adapted from ref. 50)

### 5. Conclusions and Future Studies

Overall, this study revealed that the mechanism by which TMAO induces atherogenic effects may involve histone hypomethylation. Under certain treatment conditions, TMAO induced a reduction in the trimethylation of histone H3 on lysine 27 (H3K27me3). However, the resulting TMAO-induced endothelial atherogenic phenotype was not confirmed by our cell studies. Nevertheless, we could observe in vivo the co-existence of increased plasma TMAO levels and an increased amount of atherosclerotic plaque, supporting TMAO's role in atherogenesis, but not establishing causation. Future studies will be conducted to investigate if the suppression of the epigenetic tag H3K27me3 contributes to inflammation and vascular toxicity associated with TMAO.

## Chapter 5

### REFERENCES

1. Institute of Medicine (US) Committee on a National Surveillance System for Cardiovascular and Select Chronic Diseases. Cardiovascular Disease. A Nationwide Framework for Surveillance of Cardiovascular and Chronic Lung Diseases. <https://www.ncbi.nlm.nih.gov/books/NBK83160/>. Published January 1, 1970. Accessed April 10, 2020.
2. Stewart J, Manmathan G, Wilkinson P. Primary prevention of cardiovascular disease: A review of contemporary guidance and literature. *JRSM Cardiovasc Dis*. 2017;6.
3. Roth GA, Johnson C, Abajobir A, et al. Global, Regional, and National Burden of Cardiovascular Diseases for 10 Causes, 1990 to 2015. *J Am Coll Cardiol*. 2017;70(1):1-25.
4. Heart Disease Facts. Centers for Disease Control and Prevention. <https://www.cdc.gov/heartdisease/facts.htm>. Published December 2, 2019. Accessed April 6, 2020.
5. The Editors of Encyclopaedia Britannica. Atherosclerosis. Encyclopædia Britannica. <https://www.britannica.com/science/atherosclerosis>. Published February 28, 2020. Accessed April 10, 2020.
6. Lopez EO, Jan A. Cardiovascular Disease. <https://www.ncbi.nlm.nih.gov/books/NBK535419/>. Published December 6, 2019. Last accessed April 6, 2020.
7. Anand SS, Hawkes C, de Souza RJ, et al. Food Consumption and its Impact on Cardiovascular Disease: Importance of Solutions Focused on the Globalized Food

- System: A Report From the Workshop Convened by the World Heart Federation. *J Am Coll Cardiol*. 2015;66:1590–1614.
8. Davignon J, Ganz P, Davignon J, et al. Role of Endothelial Dysfunction in Atherosclerosis. *Circulation*. 2004;109(23 Suppl 1):III27-32.
  9. Mestas J, Ley K. Monocyte-Endothelial Cell Interactions in the Development of Atherosclerosis. *Trends Cardiovasc Med*. 2008;18(6):228-32.
  10. Poston RN. Atherosclerosis: integration of its pathogenesis as a self-perpetuating propagating inflammation: a review. *Cardiovasc Endocrinol Metab*. 2019;8(2):51–61.
  11. Meerschaert J, Furie MB. The adhesion molecules used by monocytes for migration across endothelium include CD11a/CD18, CD11b/CD18, and VLA-4 on monocytes and ICAM-1, VCAM-1, and other ligands on endothelium. *J Immunol*. 1995;154(8):4099-112.
  12. Frink RJ. The Smooth Muscle Cell. The Pivot in Atherosclerosis. Inflammatory Atherosclerosis: Characteristics of the Injurious Agent. <https://www.ncbi.nlm.nih.gov/books/NBK2018/>. Accessed March 13, 2020.
  13. Moore KJ, Koplev S, Fisher EA, et al. Macrophage Trafficking, Inflammatory Resolution, and Genomics in Atherosclerosis: JACC Macrophage in CVD Series (Part 2). *J Am Coll Cardiol*. 2018;72(18):2181-2197.
  14. Rafieian-Kopaei M, Setorki M, Doudi M, et al. Atherosclerosis: process, indicators, risk factors and new hopes. *Int J Prev Med*. 2014;5(8):927–946.
  15. Anlamlert W, Lenbury Y, Bell J. Modeling fibrous cap formation in atherosclerotic plaque development: stability and oscillatory behavior. *Adv Differ Equ* 2017, 195 (2017).
  16. Bentzon JF, Otsuka F, Virmani R, Falk E. Mechanisms of plaque formation and rupture. *Circ Res*. 2014;114(12):1852-66.
  17. Desai R. Vulnerable Plaque. <http://drrajivdesaimd.com/2019/03/26/vulnerable-plaque/>. Accessed April 6, 2020.

18. Onat D, Brillon D, Colombo PC, Schmidt AM. Human vascular endothelial cells: a model system for studying vascular inflammation in diabetes and atherosclerosis. *Curr Diab Rep.* 2011;11(3):193–202.
19. Tang WW, Hazen SL. The contributory role of gut microbiota in cardiovascular disease. *J Clin Invest.* 2014;124(10):4204-11.
20. Medina-Leyte DJ, Domínguez-Pérez M, Mercado I, et al. Use of Human Umbilical Vein Endothelial Cells (HUVEC) as a Model to Study Cardiovascular Disease: A Review. *Applied Sciences.* 2020;10(3):938.
21. Getz GS, Reardon CA. Animal models of atherosclerosis. *Arterioscler Thromb Vasc Biol.* 2012;32(5):1104–1115.
22. Oppi S, Lüscher TF, Stein S. Mouse Models for Atherosclerosis Research-Which Is My Line? *Front Cardiovasc Med.* 2019;6:46.
23. Velasquez M, Ramezani A, Manal A, Raj D. Trimethylamine N-Oxide: The Good, the Bad and the Unknown. *Toxins (Basel).* 2016;8(11).
24. Janeiro MH, Ramírez MJ, Milagro FI, Martínez JA, Solas M. Implication of Trimethylamine N-Oxide (TMAO) in Disease: Potential Biomarker or New Therapeutic Target. *Nutrients.* 2018;10(10).
25. Yamashita T. Intestinal Immunity and Gut Microbiota in Atherogenesis. *J Atheroscler Thromb.* 2017;24(2):110-119.
26. Chhibber-Goel J, Singhal V, Parakh N, Bhargava B, Sharma A. The Metabolite Trimethylamine-N-Oxide is an Emergent Biomarker of Human Health. *Curr Med Chem.* 2017;24(36):3942-3953.
27. Tang WW, Hazen SL. The contributory role of gut microbiota in cardiovascular disease. *J Clin Invest.* 2014;124(10):4204-11.
28. Bennett BJ, de Aguiar Vallim TQ, Wang Z, et al. Trimethylamine-N-oxide, a metabolite associated with atherosclerosis, exhibits complex genetic and dietary regulation. *Cell Metab.* 2013;17(1):49–60.

29. Sun X, Jiao X, Ma Y, et al. Trimethylamine N-oxide induces inflammation and endothelial dysfunction in human umbilical vein endothelial cells via activating ROS-TXNIP-NLRP3 inflammasome. *Biochem Biophys Res Commun.* 2016;481(1-2):63-70.
30. Chen ML, Zhu XH, Ran L, et al. Trimethylamine-N-Oxide Induces Vascular Inflammation by Activating the NLRP3 Inflammasome Through the SIRT3-SOD2-mtROS Signaling Pathway. *J Am Heart Assoc.* 2017;6(9).
31. Ma G, Pan B, Chen Y, et al. Trimethylamine N-oxide in atherogenesis: impairing endothelial self-repair capacity and enhancing monocyte adhesion. *Biosci Rep.* 2017;37(2).
32. Boini KM, Hussain T, Li P-L, Koka SS. Trimethylamine-N-Oxide Instigates NLRP3 Inflammasome Activation and Endothelial Dysfunction. *Cell Physiol Biochem.* 2017;44(1):152-162.
33. Seldin MM, Meng Y, Qi H, et al. Trimethylamine N-Oxide Promotes Vascular Inflammation Through Signaling of Mitogen-Activated Protein Kinase and Nuclear Factor- $\kappa$ B. *J Am Heart Assoc.* 2016;5(2).
34. Cheng X, Qiu X, Liu Y, et al. Trimethylamine N-oxide promotes tissue factor expression and activity in vascular endothelial cells: A new link between trimethylamine N-oxide and atherosclerotic thrombosis. *Thromb Res.* 2019;177:110-116.
35. Ding R, Lin S, Chen D. The association of Cystathionine  $\beta$  Synthase (CBS) T833C polymorphism and the risk of stroke: a meta-analysis. *J Neurol Sci.* 2012;312(1-2):26-30.
36. Geng J, Yang C, Wang B, et al. Trimethylamine N-oxide promotes atherosclerosis via CD36-dependent MAPK/JNK pathway. *Biomed Pharmacother.* 2018;97:941-947.
37. Tan Y, Sheng Z, Zhou P, et al. Plasma Trimethylamine N-Oxide as a Novel Biomarker for Plaque Rupture in Patients With ST-Segment–Elevation Myocardial Infarction. *Circ Cardiovasc Interv.* 2019;12(1):e007281.

38. Troseid M, Ueland T, Hov JR, et al. Microbiota-dependent metabolite trimethylamine-N-oxide is associated with disease severity and survival of patients with chronic heart failure. *J Intern Med.* 2015;277(6):717-26.
39. Zhai Q, Wang X, Chen C, et al. Prognostic Value of Plasma Trimethylamine N-Oxide Levels in Patients with Acute Ischemic Stroke. *Cell Mol Neurobiol.* 2019;39(8):1201-1206.
40. Haghikia A, Li XS, Liman TG, et al. Gut Microbiota-Dependent Trimethylamine N-Oxide Predicts Risk of Cardiovascular Events in Patients With Stroke and Is Related to Proinflammatory Monocytes. *Arterioscler Thromb Vasc Biol.* 2018;38(9):2225–2235.
41. Obeid R, Awwad HM, Rabagny Y, et al. Plasma trimethylamine N-oxide concentration is associated with choline, phospholipids, and methyl metabolism. *Am J Clin Nutr.* 2016;103(3):703-11.
42. Zheng L, Zheng J, Xie Y, et al. Serum gut microbe-dependent trimethylamine N-oxide improves the prediction of future cardiovascular disease in a community-based general population. *Atherosclerosis.* 2019;280:126-131.
43. Miller CA, Corbin KD, Costa K-AD, et al. Effect of egg ingestion on trimethylamine-N-oxide production in humans: a randomized, controlled, dose-response study. *Am J Clin Nutr.* 2014;100(3):778-86.
44. Koeth RA, Lam-Galvez BR, Kirsop J, et al. l-Carnitine in omnivorous diets induces an atherogenic gut microbial pathway in humans. *J Clin Invest.* 2019;129(1):373-387.
45. Esse R, Barroso M, Tavares de Almeida I, Castro R. The Contribution of Homocysteine Metabolism Disruption to Endothelial Dysfunction: State-of-the-Art. *Int J Mol Sci,* 2019; 20(4).
46. Ea C-K, Hao S, Yeo KS, Baltimore D. EHMT1 Protein Binds to Nuclear Factor- $\kappa$ B p50 and Represses Gene Expression. *J Biol Chem.* 2012;287(37):31207-17.
47. Boers GH. Mild hyperhomocysteinemia is an independent of arterial vascular disease. *Semin Thromb Hemost.* 2000;26(3)291-295.

48. Humphrey LL, Fu R, Rogers K, et al. Homocysteine level and coronary heart disease incidence: a systematic review and meta-analysis. *Mayo Clin Proc.* 2008;83(11):1203-12.
49. Liu C, Wang Q, Guo H, et al. Plasma S-Adenosylhomocysteine is a better biomarker of atherosclerosis than homocysteine in apolipoprotein E-deficient mice fed high dietary methionine. *J Nutr.* 2008;138(2):311-315.
50. Barroso M, Kao D, Blom HJ, et al. S-adenosylhomocysteine induces inflammation through NFkB: A possible role for EZH2 in endothelial cell activation. *Biochim Biophys Acta.* 2016;1862(1):82-92.
51. Lentz SR, Sobey CG, Piegors DJ, et al. Vascular dysfunction in monkeys with diet-induced hyperhomocysteinemia. *J Clin Invest.* 1996;98(1):24-29.
52. Barroso M, Florindo C, Kalwa H, et al. Inhibition of cellular methyltransferases promotes endothelial cell activation by suppressing glutathione peroxidase 1 protein expression. *J Biol Chem.* 2014;289(22):15350-62.
53. Aranda PS, Lajoie DM, Jorcyk CL. Bleach gel: A simple agarose gel for analyzing RNA quality. *Electrophoresis.* 2012;33(2):366-369.
54. Andres-Manzano MJ, Andres V, Dorado B. Oil Red O and Hematoxylin and Eosin Staining for Quantification of Atherosclerosis Burden in Mouse Aorta and Aortic Root. *Methods Mol Biol.* 2015;1339:85-99.
55. Schindelin J, Arganda-Carreras I, Frise E, et al. Fiji: an open-source platform for biological-image analysis. *Nat Methods.* 2012;9(7):676-82.
56. Yang S, Li X, Yang F, et al. Gut Microbiota-Dependent Marker TMAO in Promoting Cardiovascular Disease: Inflammation Mechanism, Clinical Prognostic, and Potential as a Therapeutic Target. *Front Pharmacol.* 2019;10:1360.
57. Park SE, Yi HJ, Suh N, et al. Inhibition of EHMT2/G9a epigenetically increases the transcription of *Beclin-1* via an increase in ROS and activation of NF-κB. *Oncotarget.* 2016;7(26).

58. Ea CK, Hao S, Yeo KS, Baltimore D. EHMT1 protein binds to nuclear factor- $\kappa$ B p50 and represses gene expression. *J Biol Chem*. 2012;287(37):31207–31217.

## ACADEMIC VITA

### ELISABETH BACH

[bachellie.wixsite.com/ebportfolio](http://bachellie.wixsite.com/ebportfolio)  
bachellie@yahoo.com  
(717) 490-0627

#### LOCAL ADDRESS:

201 Vairo Blvd, Apt 134  
State College, PA, 16803

#### HOME ADDRESS:

7 Field Lane  
Lititz, PA, 17543

#### Education

**The Pennsylvania State University,  
Schreyer Honors College**  
*Bachelor's Degree in Nutritional Sciences  
Minor in Molecular Biology*

**University Park, Pennsylvania**  
Expected Graduation: May 2020

#### Relevant Course Experience:

- Practice in various methods of nutritional assessment
- Understanding of nutrient metabolism, molecular biology, and bodily processes
- Involvement in community nutrition outreach and nutrition education dissemination
- Knowledge of food preparation and cooking methods
- Managerial experience in large scale cooking facilities

#### Professional Experience

**Penn State Research Lab**  
*Research Assistant*

**University Park, PA**  
August 2018 to Present

- Research (currently) the interplay of hyperhomocysteinemia-induced histone hypo-methylation and atherosclerotic plaque formation
- Assist in experimental procedures
- Manage an independent research project for the lab

**State College Area School District Food Service**  
*Fulltime Intern to Food Service Manager*

**State College, PA**  
May 2019 to July 2019

- Designed nutritional infographics for school announcement screens, billboards, and menus
- Designed and coordinated student activities such as taste tests and nutrition-related games
- Prepared informative newsletters regarding nutritional issues for school administration
- Assisted in preparing and serving cafeteria food

**Café Verve**  
*Barista/Food Preparation/Cashier*

**State College, PA**  
May 2017 to September 2017

- Multi-tasked between preparing menu items, serving hot beverages, functioning as a cashier, and cleaning
- Handled up to \$500 a week in cash receipts

#### Memberships and Certifications

**ServSafe Certification**  
*Certified*

**November 2019 to Present**

**Academy of Nutrition and Dietetics**  
*Student Member*

**November 2018 to Present**